Available online at www.sciencedirect.com

SciVerse ScienceDirect

Geochimica et Cosmochimica Acta 75 (2011) 7502–7521

Geochimica et Cosmochimica Acta

www.elsevier.com/locate/gca

Nitrogen isotopes in ophiolitic metagabbros: A re-evaluation of modern nitrogen fluxes in subduction zones and implication for the early Earth atmosphere

Vincent Busigny *, Pierre Cartigny, Pascal Philippot

Institut de Physique du Globe de Paris, Sorbonne Paris Cité, Univ. Paris Diderot, UMR 7154 CNRS, 1 rue Jussieu, 75238 Paris, France

Received 17 May 2011; accepted in revised form 29 September 2011; available online 6 October 2011

Abstract

Nitrogen contents and isotope compositions together with major and trace element concentrations were determined in a sequence of metagabbros from the western Alps (Europe) in order to constrain the evolution and behavior of N during hydrothermal alteration on the seafloor and progressive dehydration during subduction in a cold slab environment (8 °C/km). The rocks investigated include: (i) low-strain metagabbros that equilibrated under greenschist to amphibolite facies (Chenaillet Massif), blueschist facies (Queyras region) and eclogite facies (Monviso massif) conditions and (ii) highly-strained mylonites and associated eclogitic veins from the Monviso Massif. In all samples, nitrogen (2.6–55 ppm) occurs as bound ammonium (NH_4^+) substituting for K or Na–Ca in minerals. Cu concentrations show a large variation, from 73.2 to 6.4 ppm, and are used as an index of hydrothermal alteration on the seafloor because of Cu fluid-mobility at relatively high temperature (>300 °C). In low-strain metagabbros, $\delta^{15}N$ values of +0.8‰ to +8.1‰ are negatively correlated with Cu concentrations. Eclogitic mylonites and veins display Cu concentrations lower than 11 ppm and show a $\delta^{15}N$–Cu relationship that does not match the $\delta^{15}N$–Cu correlation found in low-strain rocks. This $\delta^{15}N$–Cu correlation preserved in low-strain rocks is best interpreted by leaching of Cu–N compounds, possibly of the form $Cu(NH_3)_2^{2+}$, during hydrothermal alteration. Recognition that the different types of low-strain metagabbros show the same $\delta^{15}N$–Cu correlation indicates that fluid release during subduction zone metamorphism did not modify the original N and Cu contents of the parent hydrothermally-altered metagabbros. In contrast, the low Cu content present in eclogitic veins and mylonites implies that ductile deformation and veining were accompanied either by a loss of copper or that externally-derived nitrogen was added to the system.

We estimate the global annual flux of N subducted by metagabbros as 4.2 (±2.0) × 10^{11} g/yr. This value is about half that of sedimentary rocks, which suggests that gabbros carry a significant portion of the subducted nitrogen. The net budget between subducted N and that outgassed at volcanic arcs indicates that ~80% of the subducted N is not recycled to the surface. On a global scale, the total amount of N buried to the mantle via subduction zones is estimated to be three times higher than that released from the mantle via mid-ocean ridges, arc and intraplate volcanoes and back-arc basins. This implies that N contained in Earth surface reservoirs, mainly in the atmosphere, is progressively transferred and sequestered into the mantle, with a net flux of ~9.6 × 10^{11} g/yr. Assuming a constant flux of subducted N over the Earth's history indicates that an amount equivalent to the present atmospheric N may have been sequestered into the silicate Earth over a period of 4 billion years.

* Corresponding author. Address: IPGP – Bureau, 515, 1 rue Jussieu, 75238 Paris cedex 05, France. Tel.: +33 (0)1 83 95 74 34; fax: +33 (0)1 83 95 77 07.

E-mail address: busigny@ipgp.fr (V. Busigny).

0016-7037/$ - see front matter © 2011 Elsevier Ltd. All rights reserved.
doi:10.1016/j.gca.2011.09.049

1. INTRODUCTION: A BRIEF REVIEW OF NITROGEN CHEMICAL GEODYNAMICS

Nitrogen is a volatile element that can help better addressing the origin and fate of the Earth's atmosphere. This is because, unlike carbon or water, the nitrogen geodynamic cycle during mantle-surface exchanges is far from steady state. Nitrogen unsteady-state (also referred to as nitrogen disequilibrium; e.g. Boyd and Pillinger, 1994) is best illustrated by the contrasting isotope compositions of present-day degassed and recycled nitrogen, having negative and positive δ^{15}N-values of $\sim -5‰$ (where $\delta^{15}N = [^{15}N/^{14}N_{sample}/^{15}N/^{14}N_{Air} - 1] \times 1000$; Javoy et al., 1984; Marty and Humbert, 1997) and $>+2‰$ (for a review of N-isotope data in sediments, see Thomazo et al., 2009; for a discussion on the fate of nitrogen during subduction, see Bebout and Fogel, 1992; Busigny et al., 2003a,b). This predicts secular evolutions of the mantle (increasing δ^{15}N), crust and atmosphere reservoirs (decreasing δ^{15}N) through time (Javoy, 1998; Tolstikhin and Marty, 1998). Nitrogen isotope composition of the early Earth mantle would be recorded in a diamond with the lowest δ^{15}N value at $-25‰$ (Cartigny et al., 1997). Very positive δ^{15}N-values (up to 24‰) in both Archean sediments and metamorphic rocks have been interpreted to reflect the secular evolution of the atmosphere (Jia and Kerrich, 2004a) but these values contrast with other data sets illustrating very little nitrogen isotope variations of the atmosphere through time (Sano and Pillinger, 1990; Beaumont and Robert, 1999). A potential explanation might be found in the recent study of ~2.7 Gy sediments illustrating high δ^{15}N-values, up to $+50‰$, suggested to result from ammonia oxidation (Thomazo et al., 2010) rather than secular evolution of N-isotope composition in the atmosphere.

Accurately modeling the origin of the atmosphere, its chemical evolution and fate heavily relies on our knowledge of (i) N concentrations and isotope compositions in major Earth reservoirs together with (ii) fluxes between these reservoirs (e.g. Javoy, 1998; Tolstikhin and Marty, 1998; Marty and Dauphas, 2003; Jia and Kerrich, 2004a; Goldblatt et al., 2009). There is still some disagreement about present-day mantle N-contents (see Marty, 1995; Cartigny et al., 2001a, for discussion) and very few data are presently available for crustal nitrogen (Wedepohl, 1995; Boyd and Philippot, 1998; Palya et al., 2011).

Degassing and recycling fluxes are comparatively better established. Unlike noble gases which are accumulated within the Earth's atmosphere and not subducted into the mantle, nitrogen is massively recycled with a subducted/degassed ratio of ~10 (see below). This is inferred from a present-day nitrogen degassing flux at mid-ocean ridges of $\sim 0.7 \times 10^{11}$ g/yr, which is consistent with both N/He/Ar, C/N (Marty, 1995; Javoy and Pineau, 1991) and re-evaluated mantle C-flux and C/Nb-systematics (Saal et al., 2002; Cartigny et al., 2008). Secondary output fluxes are brought by back-arc basins and intraplate volcanism, which contribute, respectively, 7.8×10^9 and 5.7×10^7 g/yr (Sano et al., 2001). The flux released by arc volcanism is difficult to establish owing to the high variability of fluxes in time and space for fumaroles and volcanic gases. The value adopted here, 2.8×10^{11} g/yr, is taken from Hilton et al. (2002) as it consists of the largest database (>700 samples), contrasting with the 11 samples used for another lower estimate (8.9×10^9 g/yr; Sano et al., 2001).

The flux of N input in subduction zones can be determined from analyses of the various components of the subducting oceanic lithosphere, including sediments, basalts, gabbros and serpentinized peridotites. Analyses of metasediments in paleo-subduction zones showed that N behavior in subducting sediments is mainly controlled by the geothermal gradient (Bebout et al., 1999; Busigny et al., 2003a). Subduction along "warm" geothermal gradient (~15 °C/km) induces significant release of N from rocks to fluids (Haendel et al., 1986; Bebout and Fogel, 1992; Mingram and Bräuer, 2001), associated with N isotope fractionation (i.e. loss of ^{15}N-depleted components). In contrast, metasediments subducted along "cold" geothermal gradient (~8 °C/km) do not show any significant loss of N into fluids (Busigny et al., 2003a; Pitcairn et al., 2005). This observation reflects the high stability of N as ammonium (NH_4^+) in high-pressure white micas. The global flux of N carried by subducting metasediments was estimated to 7.6×10^{11} g/yr based on the relations between N and K abundances (Busigny et al., 2003a). This flux is three times higher than the mean flux output from arc volcanism, implying that N may be massively recycled to the mantle through subduction zones. Other fluxes, transferred by mafic and ultramafic components of the subducting oceanic lithosphere, are still missing but may contribute to surprisingly large amount of N for efficient N burial to the deep mantle (Li et al., 2007; Halama et al., 2010). Two recent studies reported N content and isotope composition of serpentinized metaperidotites from paleo-subduction zones (Philippot et al., 2007; Halama et al., 2010) and found N content between 1.4 and 15 ppm N, with very positive δ^{15}N values (+4‰ to +15‰). While this may represent a significant portion of the total N input in subduction zones, the flux of N carried by serpentinites was not assessed because the mass flux of subducting serpentinites is largely unknown. Studies of basalts drilled on the ocean seafloor have shown that alteration by seawater produces an enrichment of N in the rock (up to 18 ppm N in bulk rock) due to fluid–rock interaction (Busigny et al., 2005a; Li et al., 2007). Similar N concentrations were found in high- and ultrahigh-pressure mafic eclogites, suggesting that N stored in altered oceanic crust can be deeply and efficiently subducted (Halama et al., 2010). Again, too few data are yet available to accurately establish the N-flux related to the upper part of the oceanic crust, but increasing amount of data illustrates that these appear non-negligible compared with sedimentary flux.

In this respect, large uncertainties remain for the gabbroic part as it is the only lithological component that has not been explored so far for N concentration and isotope composition. This is a significant gap in our knowledge of the global N budget since gabbros represent 2/3 of the total mass of subducting oceanic crust, the other 1/3 being basalts (e.g. Peacock, 1990). In the present work, we report N content and isotope composition of ophiolitic gabbros from Western Alps (Europe). These rocks were em-

placed in the oceanic crust and altered by seawater-derived fluids before being subducted to various P–T conditions (blueschist and eclogite facies up to 2 GPa and 500 °C). Non-subducted equivalents were also analyzed to differentiate chemical changes related to subduction metamorphism from those related to hydrothermal circulation. Major and trace elements data were analyzed in order to determine potential co-variations with N, and constrain N geochemical behavior. In particular, the degree of Cu depletion is applied as a tracer of alteration by high-temperature hydrothermal fluids (e.g. Seewald and Seyfried, 1990; Heft et al., 2008). This unique data set is used to understand (1) the parameters controlling N concentration and isotope composition in ophiolitic metagabbros, (2) the fate of N carried by gabbros in subduction zones, (3) the flux of N deeply subducted and recycled to the mantle. Finally, the flux of N carried by subducting metagabbros is compared to other input fluxes by metasediments and metabasalts, and implications for global N geodynamic cycle and for the atmosphere evolution are discussed.

2. GEOLOGICAL SETTING AND SAMPLE DESCRIPTION

The metagabbros analyzed in this study occur together with metabasalts and metaperidotites as dismembered meta-ophiolitic bodies embedded in pelagic metasediments that form the so-called "nappe of Schistes Lustrés" of the Piemonte-Ligurian domain, western Alps (Europe; Fig. 1). These rocks experienced hydrothermal alteration on the seafloor and were in part, subsequently subducted under the Adria margin during the Late Cretaceous-Eocene in a relatively cold slab environment (~8 °C/km; Le Pichon et al., 1988; Monié and Philippot, 1989). Samples analyzed in this study include hydrothermally-altered metagabbros from the Chenaillet Massif that escaped subduction zone metamorphism (Mével et al., 1978; Manatschal et al., 2011), and blueschist- and eclogite-facies metagabbros from the Queyras region and Monviso Massif, respectively. Analyzed samples include low-strain rocks from Chenaillet, Queyras and Monviso (Fig. 2a and b) together with eclogite facies mylonites and veins from Monviso (Fig. 2c and d).

2.1. Hydrothermally-altered Chenaillet metagabbros

Chenaillet metagabbros were used as reference material predating subduction zone processes. Two samples previously investigated by Nadeau et al. (1993) for their oxygen and carbon isotope compositions were analyzed here (CH-129 and CH-80-02). These samples are undeformed metagabbros mainly composed of large crystals (mm to cm scale) of magmatic pyroxene (augite), plagioclase, apatite and ilmenite. These rocks have experienced oceanic hydrothermal alteration under greenschist- to amphibolite-facies conditions. Primary pyroxene has been partially replaced by actinolite, chlorite and green hornblende while some plagioclase has been partly pseudomorphed into epidote and calcite.

2.2. Queyras metagabbros (blueschist facies)

Four low-strain metagabbros from the Queyras region were analyzed (09-02WR, G6004A, G6004B and G6004C). The samples are mainly composed of large crystals of glaucophane (>50 vol%) in association with lawsonite and plagioclase and minor amounts of epidote, sphene and calcite (<5 vol%). Few primary magmatic pyroxenes are preserved in all samples. They are occasionally associated with rare hornblendes inherited from the hydrothermal alteration stage predating blueschist-facies overprint (samples G6004B and G6004C). Minor occurrences of secondary actinolite and chlorite pseudomorphing blueschist-facies minerals indicate that late stage retrogression under greenschist-facies conditions was limited.

2.3. Monviso metagabbros (eclogite facies)

The samples analyzed from the Monviso Massif have been subjected to extensive petrological, structural and geochemical investigations (Philippot, 1987, 1993; Philippot and Kienast, 1989; Philippot and Selverstone, 1991; Philippot and van Roermund, 1992; Nadeau et al., 1993). They belong to the Lago Superiore unit, which consists of a sequence of cumulates ranging from undifferentiated Mg–Cr metagabbros at the bottom, to more differentiated Fe–Ti metagabbros at the top (see Philippot and Kienast, 1989). In the sequence, the deformation is very heterogeneous. Strongly deformed domains with mylonitic to ultra-mylonitic textures surround low-strain domains, which preserved pre-subduction magmatic textures (Philippot and van Roermund, 1992; Nadeau et al., 1993). Highly strained domains are commonly cut across by omphacite- and garnet-bearing veins that formed during eclogite-facies metamorphism. P–T conditions estimates yield a peak pressure of about 2.5 GPa at about 550 ± 50 °C (Messiga et al., 1999). Seven well-preserved eclogitic metagabbros were selected for N isotope study. These are: two low-strain rocks (VS-1 and Vi-52), three mylonites (Vi–385M, Vi–262M and Vi–389M), and four eclogitic veins (VS–14V, Vi–79V, Vi–387V and Vi–385V). All samples contain the same omphacite (>50 vol%), garnet, rutile and apatite mineral assemblage. In addition, VS–14V contains minor talc; Vi–385V and Vi–385M, which represent a vein (V) and its adjacent mylonitic host (M), contain minor phengite (Philippot and Kienast, 1989). The low-strain Mg–Cr metagabbro (Vi-52) contains Mg–chloritoid, omphacite, spinel (chromite), talc, garnet and rutile. $\delta^{18}O$ values of omphacite between +3.0‰ to +5.3‰ (average ~+3.5‰; Nadeau et al., 1993) were attributed to be inherited from hydrothermal alteration at high temperature without subsequent re-equilibration during subduction-zone metamorphism under blueschist- and eclogite-facies conditions (Philippot et al., 1998).

3. ANALYTICAL TECHNIQUES

The procedure used for the determination of nitrogen content and isotope composition in rock samples is an improved method from Kendall and Grim (1990). It was

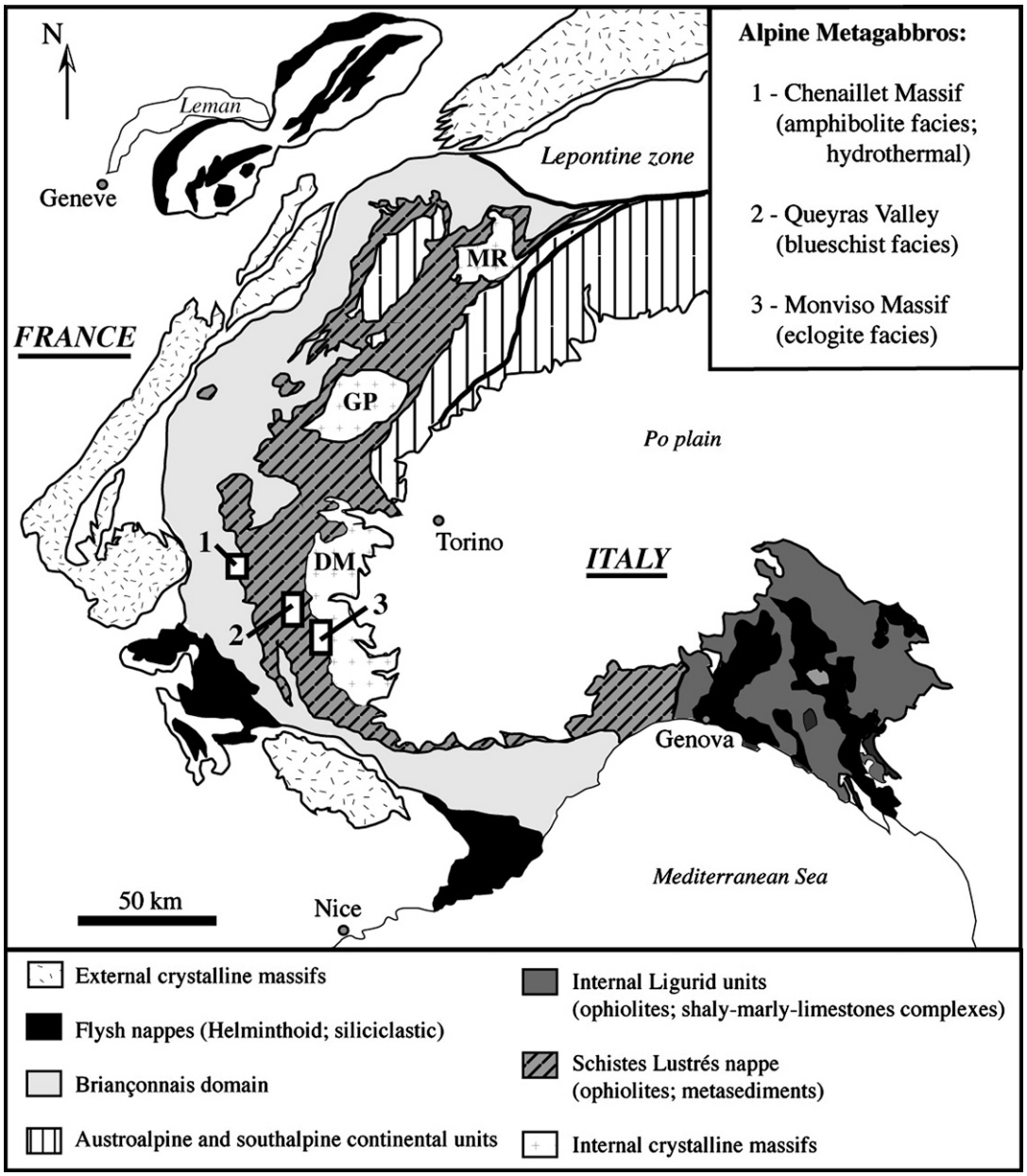

Fig. 1. Schematic map of the main tectonic units of the western Alps (modified after Agard et al., 2001). Internal crystalline massifs are from south to north: Dora Maira (DM), Grand Paradiso (GP), Monte Rosa (MR). Rectangles represent sampling zones from 1 to 3, corresponding to increasing metamorphic conditions.

thoroughly described in previous contributions (Busigny et al., 2005b; Ader et al., 2006) and is only summarized herein. Nitrogen was extracted from bulk-rock powders by combustion in quartz tubes sealed under vacuum with purified reactants (Cu, CuO and CaO). It was then quantified as N_2 by capacitance manometry in ultra-high vacuum line and its isotopic analysis was performed on a triple-collector static vacuum mass spectrometer. The N blank of the entire procedure is low (0.65 ± 0.30 nmol N), with mean $\delta^{15}N$ value of $-3.7 \pm 2.7‰$ (2σ $n = 40$; Busigny et al., 2005b). The precision for nitrogen contents and $\delta^{15}N$ values measured in our samples is better than $\pm 8\%$ and $\pm 0.5‰$, respectively.

Whole-rock major and trace elements concentrations were measured using ICP-AES and ICP-MS at the Service d'Analyses des Roches et des Mineraux (SARM) of the Centre de Recherches Petrographiques et Geochimiques (CRPG) of Vandoeuvre, France. Analytical precisions and detection limits of major and trace element concentrations are available at http://helium.crpg.cnrs-nancy.fr/SARM/pages/roches.html and are typically $\pm 10\%$.

For two samples (Vi–385V and Vi–79V), some phengites were identified and separated from their host-rock. These single phengite grains were analyzed by infrared spectroscopy using the method described in Busigny et al. (2003b,

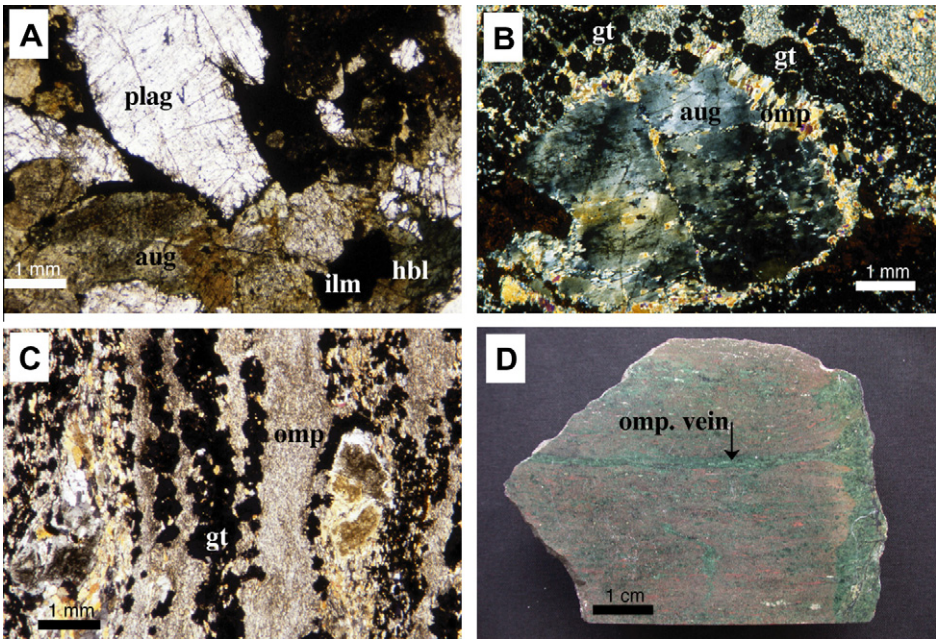

Fig. 2. Photomicrographs (A–C) illustrating the different metagabbros from the western Alps. (A) Non-subducted metagabbros from the Chenaillet massif with plagioclase (plag), augite (aug), ilmenite (ilm) and hornblende (hbl). (B) Low-strain metagabbros from the Monviso massif with large augite (aug) inherited from the magmatic paragenesis, omphacite (omp) and garnet (gt) reflect the eclogite facies of the subduction metamorphism. (C) Mylonite from the Monviso massif, showing stretched omphacite (omp) and garnet (gt). (D) Photograph of an omphacite-rich vein in an eclogite from the Monviso massif.

2004) in order to detect and, if present, quantify ammonium, NH_4^+ (substituting for K^+). Infrared spectra all show large absorption bands typical of NH_4-bending at $\sim$1430 cm^{-1} and NH_4-stretching between 2750 and 3400 cm^{-1}.

4. RESULTS

4.1. Major and trace element data

Major and trace element concentrations (Tables 1 and 2) show that the metagabbros studied represent variable degrees of magmatic differentiation. Mg# (i.e. $100 \times MgO/[MgO + FeO + Fe_2O_3]$, where MgO, FeO and Fe_2O_3 are molar abundances) is usually applied to trace magmatic differentiation because Mg/Fe ratio progressively decreases with increasing differentiation. However, our samples experienced fluid–rock interactions during hydrothermal alteration and subduction processes. Since Mg and Fe can be affected by fluid–rock exchanges (Alt, 1995; Alt and Teagle, 2003; Staudigel, 2003), Fe/Mg may have been modified and Mg# may not simply depend upon magmatic differentiation. In order to test this hypothesis, we have reported Mg# as a function of concentrations of elements, which are immobile during fluid–rock exchange (e.g. HFSE, REE; Staudigel, 2003; Spandler et al., 2004). Incompatible and fluid-immobile elements like Zr, Hf, Nb (HFSE) and Lu (REE) show an increasing concentration with decreasing Mg# (Fig. 3). On the contrary, Cr, which is a compatible element, shows a progressive decrease over several orders of magnitude (from 7.3 to 17,900 ppm) with decreasing Mg# (Fig. 3). These correlations indicate that Mg# was only moderately affected by hydrothermalism and subduction (e.g. Staudigel, 2003). Thus major elements primarily reflect magmatic processes at mid-ocean ridges. Other major elements such as Fe, Mn, and Ti show increasing concentrations with decreasing Mg# (Fig. 3), reflecting the well-known incompatible behavior of Fe, Mn and Ti relative to Mg. Cu content of low-strain metagabbros show a wide range of variation (from 6.4 to 73.2 ppm) and tends to correlate with Mg# (except for the Mg-rich metagabbro). Veins and mylonites have low Cu concentrations (less than 11 ppm for all samples but one vein with 27 ppm). Aluminum concentration roughly decreases, reflecting its compatible behavior during plagioclase crystallization. These chemical features can be used to distinguish two groups of gabbros, being either Mg–Cr rich or Fe–Ti rich rocks (Lombardo et al., 1978). Since the gabbros are cumulates, they could not necessarily fall on differentiation trends. For example, some rocks could contain intercumulus melt and be enriched in incompatible elements, or others could be depleted in incompatible elements (e.g. Alt and Anderson, 1991). However, the present data generally show reasonable igneous trends while some variability may be explained by the fact that the rocks are cumulates.

4.2. Nitrogen concentration and isotope composition

Tables 3 and 4 report N concentrations and isotope compositions of whole-rock samples for low-strain metagabbros, mylonites and veins, respectively. All but one sample were analyzed at least twice and show a very good reproducibility (within $\pm 0.5‰$). Among the four

Table 1
Major and trace element concentrations in Alpine undeformed and low-strain metagabbros.

Samples	CH-129	CH-80-02	G6004A	G6004B	G6004C	09-02WR	VS-1	Vi-52
SiO_2	41.76	34.69	48.27	47.05	50.07	53.43	45.44	43.60
Al_2O_3	11.90	8.69	19.86	11.37	8.48	13.16	12.72	20.02
Fe_2O_3	16.90	21.61	7.31	16.73	16.11	9.06	14.93	4.61
MnO	0.29	0.37	0.13	0.27	0.19	0.14	0.21	0.05
MgO	4.73	5.20	3.31	5.91	5.06	9.48	6.34	13.44
CaO	11.69	14.66	9.57	7.08	5.64	4.93	10.66	9.91
Na_2O	3.66	2.78	4.87	4.78	5.75	5.66	3.91	2.40
K_2O	–	0.05	–	–	–	–	0.02	–
TiO_2	2.96	6.00	0.70	4.25	6.28	0.50	6.40	0.17
P_2O_5	4.10	5.49	0.12	0.64		0.04	0.09	0.05
LOI	1.49	0.54	4.39	2.32	0.90	3.23	0.83	3.59
Total	99.48	100.08	98.53	100.40	98.48	99.63	99.87	97.84
Ce	82.6	82.8	3.4	17.1	1.8	1.8	1.2	
Co	28.9	48.9	20.4	41.4	47.4	32.4	22.1	48.8
Cr	12.6	7.3	30.3	10.6	9.8	129	113	17,900
Cs	–	–	0.3	–	–	–	–	–
Cu	49.3	73.2	33.6	45.4	41.3	6.4	22.5	60.3
Dy	28.3	29.4	2.3	10.8	2.5	1.8	3.7	–
Er	13.5	13.8	1.4	5.9	1.7	1.1	2.3	–
Eu	7.5	7.5	0.9	2.4	0.7	0.6	0.3	–
Ga	17.3	14.4	20.7	20.1	12.1	12.3	–	13.0
Gd	33.6	35.2	2.0	10.0	1.7	1.5	1.2	–
Ge	1.6	1.8	1.8	1.5	2.1	1.0	–	1.0
Hf	1.2	1.4	0.9	2.8	1.4	0.6	2.1	0.2
Ho	5.5	5.6	0.5	2.2	0.5	0.4	1.0	–
In	0.1	0.1	0.1	0.2	0.1	–	–	0.1
La	24.9	23.8	1.9	4.9	0.6	0.5	0.3	
Lu	1.3	1.3	0.2	0.8	0.3	0.2	0.4	–
Mo	0.9	0.8	0.6	0.9	0.4	–	–	0.6
Nb	2.4	2.6	0.3	2.6	2.3	0.1	2.5	0.1
Nd	91.4	92.9	4.1	21.0	2.5	2.3	1.4	–
Ni	27.5	40.8	99.4	13.5	75.8	72.2	46.3	477
Pb	4.2	–	8.2	6.1	6.6	–	–	–
Pr	16.1	15.9	0.8	3.5	0.4	0.4	0.2	
Rb	–	–	4.2	0.8	–	0.6	2.9	–
Sm	27.9	29.0	1.4	7.6	1.2	1.0	0.7	–
Sn	3.9	1.4	0.6	1.1	2.2	0.4	–	0.5
Sr	175	131	123	87.2	34.4	101	36.8	14.3
Ta	0.2	0.3	–	0.2	0.2	–	–	–
Tb	5.0	5.1	0.3	1.7	0.4	0.3	0.4	
Th	0.1	0.1	–	0.1	0.0	–	–	–
Tm	1.7	1.7	0.2	0.8	0.3	0.2	0.4	–
U	0.1	0.1	0.1	–	0.1	–	–	–
V	69.5	381	256	447	692	166	699	102
W	2.8	0.9	0.6	1.0	0.5	0.3	–	1.6
Y	170	173	13.5	59.4	15.4	10.4	24.2	0.2
Yb	9.7	9.5	1.4	5.4	2.1	1.0	2.2	0.0
Zn	118	139	60.5	131	114	56.1	86.5	90.5
Zr	47.3	57.6	32.7	106	55.1	17.3	80.8	6.8

Major and trace element concentrations are, respectively, in wt% and ppm.

high-pressure veins studied, two contain minor amounts of phengite (Vi–385V and Vi–79V). Estimates of the phengite NH_4^+ concentrations by infrared spectroscopy yielded 584 ± 37 ppm (2σ, $n = 5$) and 1046 ± 70 ppm (2σ, $n = 3$) for the two samples, respectively.

Nitrogen amounts for mass spectrometer measurements range from 7 to 124 nmol N, which are more than 10 times higher than the average blank. With the exception of one eclogitic vein (VS–14V) that contains 55 ppm nitrogen (Table 4), whole-rock N contents range between 2.6 and 28 ppm. The N content of low-strain metagabbros shows a rough positive correlation with the sum of $CaO + Na_2O$ concentrations (Fig. 4), which is used as a proxy of the amount of Ca–Na-bearing crystals in the samples (feldspars or augite in gabbros; sericite, zeolite, hornblende in hydrothermally-altered metagabbros; clinopyroxene in eclogitic metagabbros). $\delta^{15}N$ values vary from +0.8‰ to +8.1‰, a range strikingly similar to that of HP/UHP eclogites

Table 2
Major and trace element concentrations in mylonites and veins.

Samples	Vi–262M	Vi–389M	Vi–385M	Vi–385V	Vi–387V	Vi–79V	VS–14V
SiO_2	42.94	43.06	47.19	44.81	54.07	46.09	52.45
Al_2O_3	13.09	12.93	11.71	13.01	5.15	8.83	8.65
Fe_2O_3	19.60	20.33	15.94	17.85	9.94	9.25	10.80
MnO	0.33	0.41	0.31	0.38	0.11	0.07	0.05
MgO	4.82	4.94	5.46	5.06	9.22	7.64	7.71
CaO	10.27	8.17	9.49	9.26	15.00	14.58	10.40
Na_2O	4.32	4.12	5.21	4.73	5.86	5.19	7.05
K_2O	0.03	–	0.20	0.30	–	0.04	–
TiO_2	2.99	6.67	4.53	4.30	0.07	2.81	0.64
P_2O_5	1.93	0.74	0.24	0.82		3.15	0.21
LOI	–	–	–	–	0.48	0.93	0.77
Total	99.39	100.35	100.00	99.99	99.90	98.54	98.73
Ce	39.2	23.1	11.2	22.1	0.2	42.3	33.0
Co	23.2	15.7	23.0	27.5	12.4	19.1	35.1
Cr	15.9	12.5	8.0	12.6	1141	743	1007
Cs	–	–	–	–	–	–	–
Cu	7.8	8.7	9.2	8.6	9.3	27.8	11.1
Dy	16.3	14.7	8.1	11.8	0.5	7.1	3.0
Er	9.2	8.6	4.6	6.3	0.5	1.8	0.8
Eu	5.3	3.0	1.3	2.2	0.1	7.1	3.2
Ga	22.3	19.6	21.0	21.5	12.1	20.1	22.9
Gd	18.6	12.1	6.2	10.1	0.2	20.2	8.3
Ge	2.1	1.9	1.6	1.9	1.3	1.2	1.2
Hf	6.7	3.8	2.6	2.8	0.2	4.7	1.0
Ho	3.3	3.0	1.7	2.3	0.1	0.9	0.4
In	0.2	0.1	0.2	0.2	0.1	0.1	0.1
La	9.5	6.6	3.2	6.3	0.1	8.3	10.7
Lu	1.2	1.2	0.7	0.8	0.1	0.2	0.1
Mo	0.6	0.6	–	0.6	–	0.5	0.7
Nb	3.4	6.7	3.2	3.2	0.5	3.3	0.7
Nd	48.9	24.5	11.0	22.4	0.3	67.2	33.1
Ni	19.1	34.8	33.3	23.3	484	155	297
Pb	22.6	–	–	–	–	–	–
Pr	8.2	4.3	2.0	4.1	–	10.1	6.1
Rb	–	0.7	6.7	7.1	–	1.1	2.3
Sm	17.0	8.3	3.8	7.2	0.1	24.9	9.8
Sn	1.5	1.6	1.5	1.5	1.9	1.3	1.2
Sr	217	77.8	55.5	56.8	12.2	198	59.7
Ta	0.3	0.6	0.3	0.3	–	0.3	0.1
Tb	2.7	2.2	1.2	1.8	0.1	1.9	0.8
Th	0.1	0.1	0.1	0.1	0.4	–	0.1
Tm	1.3	1.2	0.7	0.9	0.1	0.2	0.1
U	0.1	–	0.1	0.1	0.2	–	–
V	421	492	616	619	98.8	350	301
W	0.5	0.4	0.7	0.7	0.4	0.3	0.5
Y	97.5	88.8	46.5	70.6	3.5	23.8	9.3
Yb	8.1	8.1	4.6	5.6	0.6	1.1	0.5
Zn	132	135	123	130	111	108	119
Zr	359	149	93.3	120	6.9	196	37.7

Major and trace element concentrations are respectively in wt% and ppm.

(−1‰ to +8‰; Halama et al., 2010). Nitrogen concentration tends to decrease with increasing $\delta^{15}N$ value (Fig. 5a) independently of the metamorphic grade. This decrease is also observed when N concentration is normalized to the concentration of fluid-immobile elements such as Al and Zr (Fig. 5b and c). In low-strain metagabbros, with the exception of sample Vi-52, both $\delta^{15}N$ values and Cu concentrations appear correlated with the Mg# (Fig. 3). The recognition that Cu concentrations and $\delta^{15}N$ values of low-strain metagabbros are strongly correlated (Fig. 5d, $r^2 = 0.96$) indicates that N and Cu geochemical behaviors were controlled by a common process. Cu/Al and Cu/Zr molar ratio of low-strain metagabbros are also roughly correlated with $\delta^{15}N$ (Fig. 5e and f). In contrast, mylonites and veins plot significantly below the trend defined by the low-strain metagabbros (Fig. 5d, e and f). Among all the elements analyzed (reported in Tables 1 and 2), Cu is the only one to show a significant correlation with $\delta^{15}N$.

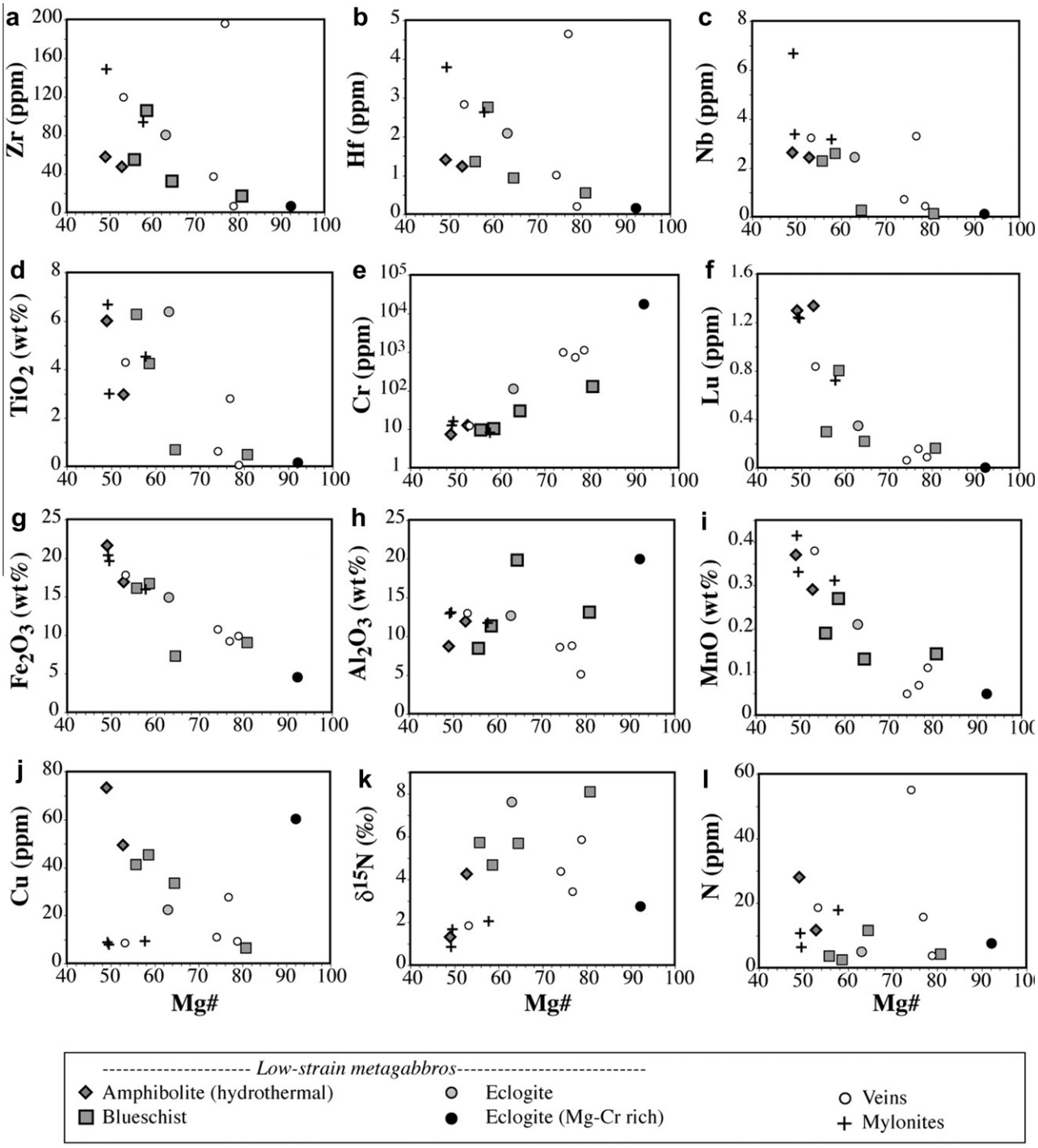

Fig. 3. Selected major and trace element concentrations reported as a function of Mg# (Niggli Mg# = 100 × MgO/(MgO + FeO + Fe_2O_3), where MgO, FeO and Fe_2O_3 are molar abundances) for Alpine metagabbros analyzed in this study. This illustrates that our sample set represent variable degrees of magmatic differentiation from Mg–Cr-rich to Fe–Ti-rich endmembers.

5. DISCUSSION

5.1. Nitrogen speciation in Alpine metagabbros

The determination of N speciation in metagabbros is difficult because N occurs in trace amounts (ppm level) and no N-bearing phases can be readily identified (except for the few secondary phengites present in eclogitic veins Vi–385V and Vi–79V). In situ techniques such as electron microprobe (Beran et al., 1992), ion microprobe (Hashizume et al., 2000) or nuclear reaction analyses (Gallien et al., 2004; Orberger et al., 2005) so far cannot resolve concentrations below

Table 3
Results of N analysis for undeformed and low-strain Alpine metagabbros.

Sample	Microstructure	Weight (mg)	N amount (nmol)	N content (ppm)	$\delta^{15}N$ (‰)
Chenaillet					
Amphibolite facies Fe-metagabbros (hydrothermal)					
CH-129	Undeformed	39.75	34	11.9	3.8
CH-129		32.88	27	11.4	4.7
			Avg.	11.7	4.3
CH-80-02	Undeformed	10.64	20	26.1	1.5
CH-80-02		28.94	62	29.9	1.2
			Avg.	28.0	1.3
Queyras					
Blueschist facies Fe-metagabbros					
G6004A	Low-strain	44.11	38	11.7	6.1
G6004A		35.56	30	11.6	5.3
			Avg.	11.6	5.7
G6004B	Low-strain	36.78	7	2.6	4.8
G6004B		38.79	8	2.6	4.6
			Avg.	2.6	4.7
G6004C	Low-strain	38.41	10	3.6	5.9
G6004C		44.24	13	3.8	5.5
			Avg.	3.7	5.7
09-02WR	Low-strain	30.96	9	4.0	8.0
09-02WR		31.82	11	4.6	8.0
09-02WR		35.52	12	4.5	8.4
			Avg.	4.4	8.1
Monviso					
Eclogite facies Fe-metagabbro					
VS-1	Low-strain	30.80	12	5.1	7.9
VS-1		40.37	15	5.1	7.4
			Avg.	5.1	7.6
Eclogite facies Mg-metagabbro					
Vi-52	Low-strain	30.93	17	7.6	2.5
Vi-52		34.56	20	7.9	3.0
			Avg.	7.7	2.8

Table 4
Results of N analysis for mylonites and veins from the Monviso massif.

Sample	Microstructure	Weight (mg)	N amount (nmol)	N content (ppm)	$\delta^{15}N$ (‰)
Vi–262M	Mylonite	34.36	16	6.2	1.7
Vi–262M		54.34	26	6.5	1.7
			Avg.	6.3	1.7
Vi–389M	Mylonite	67.56	52	10.6	0.8
Vi–385M	Mylonite	58.38	75	17.8	2.0
Vi–385V	Vein	29.00	40	19.0	2.0
Vi–385V		39.91	53	18.5	1.7
			Avg.	18.7	1.9
Vi–387V	Vein	36.13	10	3.8	5.2
Vi–387V		40.49	12	4.0	6.5
			Avg.	3.9	5.9
Vi–79V	Vein	13.77	16	15.8	4.0
Vi–79V		20.07	23	15.9	2.9
			Avg.	15.9	3.4
VS–14V	Vein	9.47	39	57.2	4.0
VS–14V		32.50	124	53.1	4.7
			Avg.	55.1	4.4

few hundreds of ppm. Consequently, in the present work, N speciation is assessed indirectly. A first observation is that N concentrations reported in this study represent N fixed/bound in minerals – not in fluid inclusions – because N was extracted from fine powders (<60 μm) initially degassed under vacuum at 450 °C (see Section 3). This is consistent with results of the fluid inclusion analysis performed in omphacite from Monviso metagabbros, which showed that

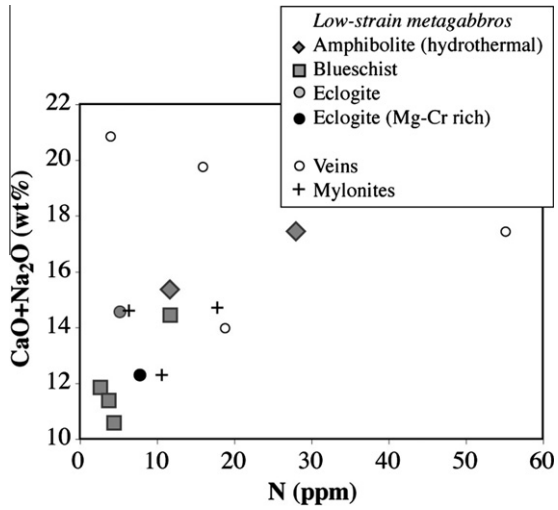

Fig. 4. Concentrations of $CaO + Na_2O$ (in wt%) reported vs N content (in ppm) for Alpine metagabbros. Low-strain metagabbros show a rough positive correlation, supporting that N likely occurs as NH_4^+ in Ca–Na minerals.

the inclusion fluid is devoid of nitrogen (Philippot and Selverstone, 1991). Nitrogen bound in crustal rocks usually occurs as ammonium, NH_4^+ (e.g. Vedder, 1964, 1965; Yamamoto and Nakahira, 1966). Ammonium is substituting for K^+ in K-bearing minerals such as feldspars and micas but can also occur in plagioclase feldspars substituting for Ca and Na (Honma and Itihara, 1981). In Alpine metagabbros, K concentrations are particularly low, generally below the analytical detection limit (i.e. <0.05 wt%). Petrological study of our samples indicates that K-bearing minerals are virtually absent. Nitrogen in Alpine metagabbros is thus believed to reside as NH_4^+ in Ca–Na-bearing minerals. Low-strain metagabbros show a crude correlation between N content and $Na_2O + CaO$ content, supporting this idea (Fig. 4).

For the two veins where phengite was identified and separated (Vi–385V and Vi–79V), infrared spectroscopy analysis shows that they contain large amounts of ammonium (>500 ppm in single grains). This indicates that N primarily occurs as NH_4^+ in these veins. In contrast, the vein labeled VS–14V does not contain any phengite although its bulk-rock N content is the highest measured (~55 ppm N), indicating that nitrogen is carried by another phase. The mineralogy of this sample is dominated by omphacite, with minor talc and garnet. Interestingly, it also contains the highest Na content analyzed, suggesting that N may reside as NH_4^+ in the Na^+ crystallographic site. In support of this statement, infrared spectroscopy analyses of paragonite (i.e. Na white mica) separates from metasediments have NH_4^+ concentrations up to 120 ppm, showing that

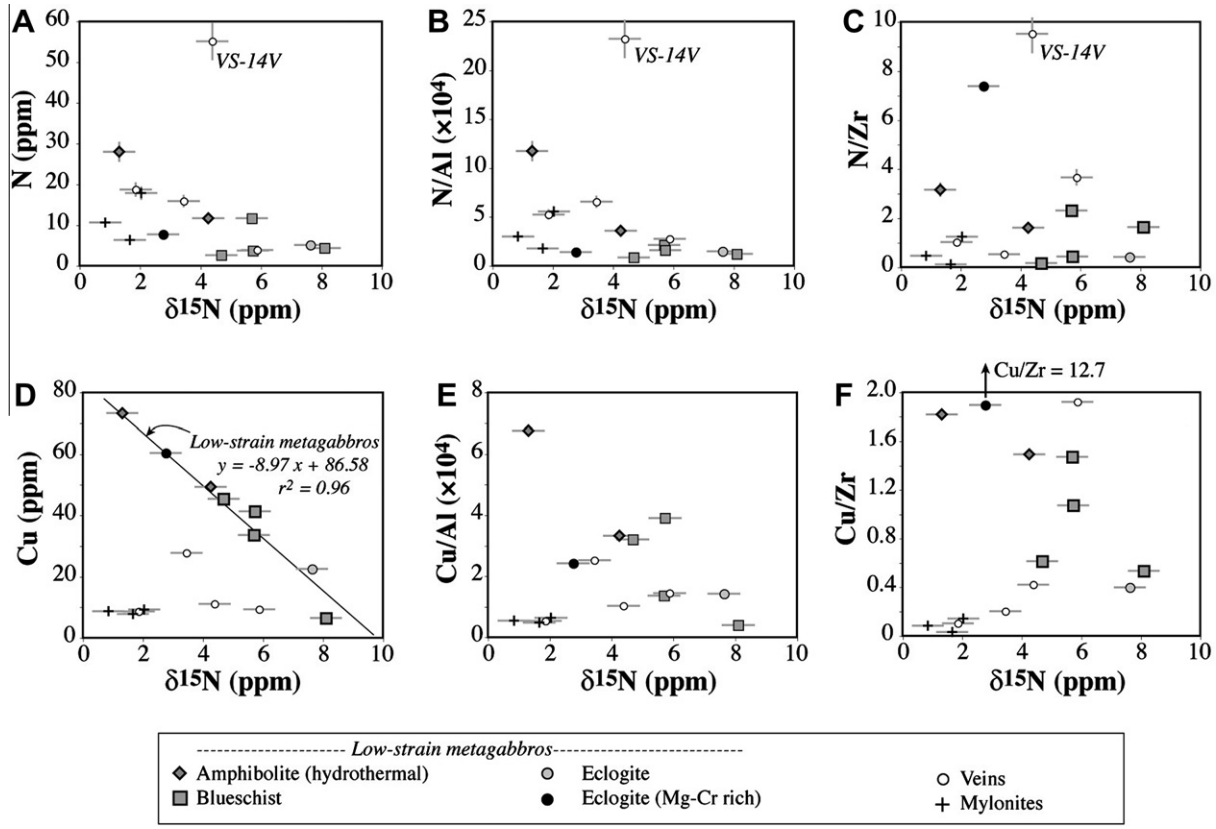

Fig. 5. Nitrogen concentration, N/Al and N/Zr molar ratios, and Cu concentrations together with Cu/Al and Cu/Zr molar ratios as a function of N isotope compositions in Alpine metagabbros. (A–C) N content, N/Al and N/Zr tend to decrease with increasing $\delta^{15}N$. (D–F) Low-strain metagabbros show an inverse linear relationship between Cu content and $\delta^{15}N$, also observed in Cu/Al and Cu/Zr molar ratios vs $\delta^{15}N$.

Na-bearing minerals can contain significant amount of N as ammonium, in agreement with the study of Honma and Itihara (1981). Accordingly, available evidence is consistent with N occurring mainly as NH_4^+ in Ca–Na minerals in low-strain metagabbros and in phengite in some high-pressure veins. The occurrence of NH_4^+ in mafic and ultramafic rocks is in full agreement with the recent conclusions from high-pressure experiments on clinopyroxene (Watenphul et al., 2009, 2010) and a study on mantle peridotite xenoliths (Yokochi et al., 2009).

5.2. Significance of the relationship Cu–δ^{15}N

Low-strain metagabbros show an inverse linear correlation between Cu concentration and δ^{15}N (Fig. 5d). This correlation could be inherited from (i) magmatic crystallization and differentiation, (ii) oceanic hydrothermalism or (iii) Alpine subduction process. These three hypotheses are discussed in details bellow.

Two samples from the Chenaillet massif, which have not been buried in a subduction zone, define a correlation indistinguishable from the one defined by subducted metamorphic rocks (Fig. 5d). This observation implies that the Cu–δ^{15}N relationship was acquired before the subduction stage either during magmatic differentiation or oceanic hydrothermalism. This idea is also supported by the fact that the Cu–δ^{15}N correlation does not show any progressive trend with increasing metamorphic grade (from non-subducted to blueschist- and eclogite-facies rocks).

With regards to magmatic differentiation, while N isotope composition may reflect magma degassing or variation in N speciation related to melt oxygen fugacity, Cu content distribution might be the expression of sulfide saturation and crystallization. Indeed, copper usually behaves as an incompatible element during differentiation of basaltic magmas (Brügmann et al., 1993; Alirezaei and Cameron, 2002), thus being progressively concentrated in the residual melt (Hamlyn et al., 1985) except if the magma reaches sulfur saturation. In the latter case, Cu behaves compatibly with respect to sulfide, resulting in a residual melt that is progressively becoming more depleted with respect to Cu and Mg. A compilation of data for mid-ocean ridge basalts shows a positive correlation between Cu and MgO contents (Fig. 6a; data from PetDB database, http://www.petdb.org/), illustrating that significant amount of Cu is stored by sulfides precipitated during magmatic differentiation. In Fig. 6, Alpine metagabbros are compared to MORB data. Comparing MORB and gabbros may not be straightforward because the gabbros are cumulates whereas the lavas represent melt compositions affected by variable degrees of differentiation. Gabbros can contain intercumulus melt (liquid) or could be cumulates from which such differentiated melt has been excluded (e.g. Alt and Anderson, 1991). In the case of Alpine metagabbros, relationships between Cu and MgO (Figs. 3j and 6a) and between Zn/Cu and MgO (Fig. 6b) are outlined. The overlap with MORB data (same Figures) suggests their comparison is meaningful. In Fig. 6a, Alpine metagabbros plot in part on the correlation defined by MORB, but it is not clear whether sulfide saturation was reached or not. Zinc is another incompatible element, which, compared to copper, is poorly partitioned into sulfide. The residual melt displays a negative correlation between Zn and MgO (not shown) and thus a positive correlation of Cu/Zn ratio with MgO (see MORB compilation in Fig. 6b). Fig. 6b shows that low-strain metagabbros define a single trend (except for one sample) that is inverse relative to the correlation defined by MORB. This indicates that during gabbro crystallization, sulfide saturation was not reached. Only one metagabbro with the highest MgO (13.44 wt%) appears comparatively enriched in Cu compared to other samples and might reflect sulfide accumulation (Fig. 6b).

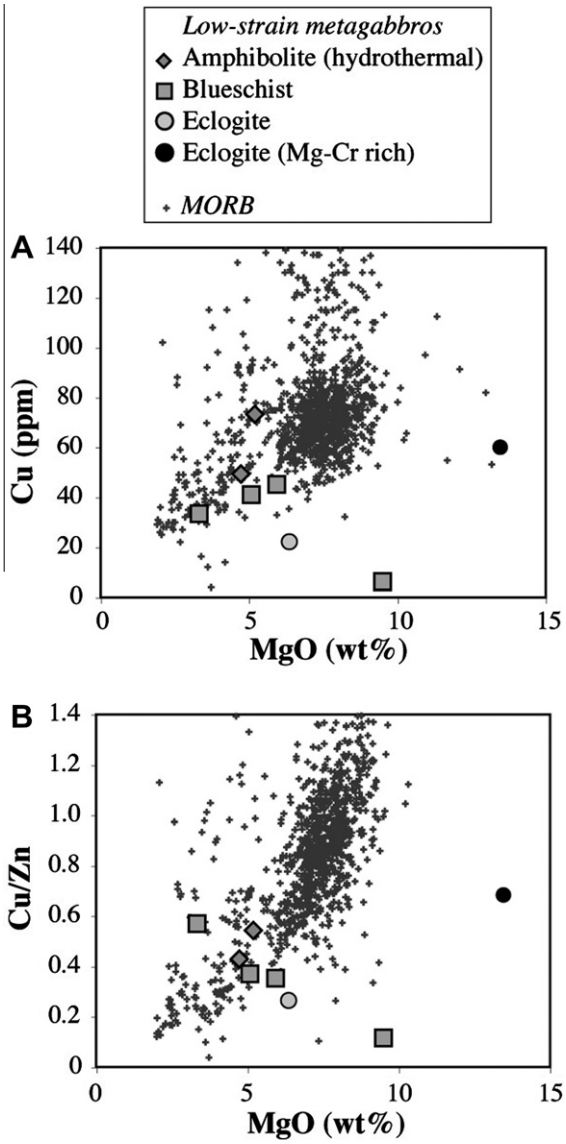

Fig. 6. Copper concentration and Cu/Zn molar ratio vs MgO content for low-strain Alpine metagabbros. A compilation for mid-ocean ridge basalts (MORB) is shown for comparison (data from PetDB database, http://www.petdb.org/). Data reported for MORB are glasses with MgO content >2 wt% and represent various settings all over the world (including Indian, Atlantic and Pacific mid-ocean ridges).

Magmatic differentiation is unlikely to account for the $\delta^{15}N$–Cu relationship for at least three other reasons:

(1) The normalization of Cu concentration to fluid-immobile elements such as Al and Zr (for which variations of concentration are only related to magmatic processes) also show negative correlations with $\delta^{15}N$ (Fig. 5e and f). This indicates that variations of Cu concentration are mostly controlled by secondary process (i.e. non magmatic). Contrasting with Al and Zr, Cu was added or lost from the rock by an interaction with a fluid.

(2) Based on available experiments, it can be inferred that nitrogen is likely dissolved as N_2 in basaltic melt for oxygen fugacities ranging between IW (Iron–Wustite) to Air (e.g. Libourel et al., 2003; Roskosz et al., 2006). However, these studies were undertaken in anhydrous conditions and the occurrence of NH_3 might actually be more significant than determined experimentally. For example, under high f_{H_2}, amine groups (e.g. NH_3, NH_2^-) are formed and stabilized (Mysen et al., 2008; Mysen and Fogel, 2010), and significant N-content and isotopic variations could be produced if nitrogen partitioning between melt and sulfide (and/or co-precipitating Ca–Na minerals) is important, leading to a decrease of N concentration in the magma with increasing differentiation. However, to our knowledge, the presence of NH_4^+ in magma has never been observed. This assumption is also at odd with the overall enrichment in N with decreasing Mg# reported in Fig. 3l.

(3) Large N-isotope fractionation could also be recorded in the residual melt if nitrogen partitioning between melt and sulfide (and/or co-precipitating Ca–Na minerals) was significant, in particular if nitrogen was stored as ammonium. This process would produce a decrease of the magma N concentration together with an increase of $\delta^{15}N$ due to isotope exchange between reduced and oxidized N species of <3‰ (e.g. the isotope fractionation factor $\alpha_{NH_4-N_2}$ is <1.0032 for temperature higher than 930 °C; Scalan, 1957; Richet et al., 1977; Hanschmann, 1981; Haendel et al., 1986). If we assume that magmatic N_2 had $\delta^{15}N$ ~−5‰ typical of mid-ocean ridge basalt values (Javoy and Pineau, 1991; Marty and Humbert, 1997; Marty and Zimmermann, 1999; Cartigny et al., 2001b), NH_4^+ should have $\delta^{15}N$ values between −5‰ and −2‰. This result contrasts with our dataset since rock samples with low N content (that would represent magma with low NH_4^+ content and high N_2 content) all show $\delta^{15}N$ >+4‰ (Fig. 5a).

The scenario about magmatic differentiation can be regarded with few modifications assuming that N was degassed during progressive differentiation. A loss of N_2 from the melt by degassing could produce a shift of N isotope composition if Rayleigh distillation process was associated with an isotope exchange between exsolved N_2 and dissolved N_2 (about −1.2‰; Cartigny et al., 2001b) or NH_4^+ (about 3‰; Scalan, 1957). A degassing of N_2 from the magma would progressively decrease N content and increase $\delta^{15}N$ value of the residual N in the melt. Following this model, N content decrease and $\delta^{15}N$ increase should be correlated with a decrease of Mg#, which tracks magma differentiation. Fig. 3k and l shows the opposite in low-strain metagabbros since $\delta^{15}N$ decreases with decreasing Mg# and increasing N contents. In other words, the lowest $\delta^{15}N$ values and highest N contents are observed for the most differentiated samples.

The only alternative that can account for the Cu–$\delta^{15}N$ linear correlation recorded in low-strain gabbros is a hydrothermal origin. Because samples with the highest N contents also show the highest Cu content (and *vice versa*), we suggest that N and Cu behave similarly, being either added to or leached from the rock by the circulating fluid. Experimental studies and analyses of altered oceanic crust both show that hydrothermal fluids with temperature >300 °C and moderate water–rock ratio can mobilize substantial amounts of Cu (e.g. Seewald and Seyfried, 1990; Heft et al., 2008). By inference, this is also compatible with the idea that N is a fluid-mobile element (e.g. Bebout, 1995). Given the lower amounts of Cu in our metagabbros compared to most fresh MORB (Fig. 6a), it is likely that Cu and N were rather mobilized and leached out of the rock rather than added. This is also evidenced by the decrease of N/Al and Cu/Al ratio with increasing $\delta^{15}N$ (Fig. 5), because Al is an immobile element during fluid–rock interaction. Although not exclusive, the simplest scenario that can be considered is the formation of copper(II) complexes with ammonia in the fluid. Copper(II) complexes with ammonia can be written as $Cu(NH_3)_X^{2+}$, where x varies mainly from 1 to 4 (e.g. Bjerrum, 1941). The formation of $Cu(NH_3)_X^{2+}$ complexes can strongly increase the solubility of both Cu and N in hydrothermal fluids. While N_2 can also be present in hydrothermal systems (e.g. Bottrell et al., 1988; Yardley et al., 1993), it is not considered further in the discussion because N_2 should not form any chemical complex with Cu. An important question is whether NH_3 can be stable under pH and P–T conditions attending hydrothermal conditions similar to those experienced by Alpine metagabbros. The transformation of NH_4^+ to NH_3 is an acid–base reaction written as:

$$NH_4^+ \rightarrow NH_3 + H^+$$

The pK_A of this reaction is lower than 4.8 at temperature higher than 300 °C (Olofsson, 1975). For conditions typical of high-temperature hydrothermalism (i.e., a fluid with pH >5 and amphibolite facies PT conditions), the dominant N species in the fluid will be NH_3 and therefore NH_4^+ can be partitioned from the rock to the fluid. NH_4^+ can be immediately transformed to NH_3, and NH_3 can react with Cu to form $Cu(NH_3)_X^{2+}$. In this model, Cu solubility is enhanced by NH_3 concentration, which in turn tends to scavenge Cu from the rock. In order to test quantitatively this hypothesis, we have modeled the evolution of Cu and N concentrations together with $\delta^{15}N$ during leaching by hydrothermal fluids. Choosing an initial $\delta^{15}N$ value of −5‰ for the reference gabbro prior to leaching would lead to initial Cu and N contents of >250 and 100 ppm, respectively. Such high Cu and N concentrations are not compatible with typical mantle-derived magma (e.g. for N see Marty, 1995; for Cu see Fig. 6a). For this reason, we have assumed that the sample CH80-02, which contains the highest N and Cu concentrations (28 ppm N and 73 ppm Cu) and the lowest $\delta^{15}N$ value among low-strain metagabbros (+1.3‰), is representative of initial conditions. These initial values are different from typical mantle-derived melt; N content

(28 ppm N) is about 10 times higher and $\delta^{15}N$ (+1.3‰) is at least 3‰ higher than basaltic melts. The origin of these high N content and $\delta^{15}N$ values is unclear but may arise from (i) a moderately-compatible behavior of N during gabbro crystallization, potentially with N isotope fractionation between crystal and melt, and/or from (ii) melt-assimilation of deep crustal material enriched in N by seawater–rock interaction. Using the metagabbro CH80-02 as a starting point, two different calculations were performed considering (1) a Rayleigh distillation model or (2) a batch equilibrium model. Similar models were used in previous studies to simulate N isotope fractionation during fluid release associated with subduction of metasediments (e.g. Bebout and Fogel, 1992; Mingram and Bräuer, 2001). In our first model, we assumed that N occurred as NH_4^+ (see Section 5.1) and was progressively transformed and lost as NH_3 in the fluid. Assuming that each small aliquot of NH_3 produced was immediately transferred out of the system, the effect of N loss from the rock on its stable isotope composition can be modeled as Rayleigh distillation. The Rayleigh distillation describes an exponential enrichment of ^{15}N over ^{14}N in the residual NH_4^+ in the rock that is calculated as:

$$\delta^{15}N_{NH_4} = \delta^{15}N^0_{NH_4} + 1000(\alpha - 1)\ln F$$

where $\delta^{15}N^0_{NH_4}$ and $\delta^{15}N_{NH_4}$ represent the initial and residual N-isotope composition of the rock, F is the N fraction remaining in the rock and α is the fractionation factor between NH_3 in the fluid and NH_4. We assumed that the N isotope fractionation between NH_3 and $Cu(NH_3)_X^{2+}$ was negligible. Fig. 7a shows that N isotope fractionation between NH_4^+ remaining in the rock and NH_3 leaving the system produces an increase of $\delta^{15}N$ value in the residual rock. However, in Cu–$\delta^{15}N$ and N–$\delta^{15}N$ diagrams, the predicted $\delta^{15}N_{NH_4}$ increases exponentially with decreasing Cu and N contents. This contrasts with the present data, which rather shows a linear correlation in a Cu–$\delta^{15}N$ diagram (Fig. 5d). No combination was able to produce a good fit to the data, whatever the initial conditions (Cu and N contents, $\delta^{15}N$) and $\alpha_{NH_3-NH_4}$, and x-values (i.e. in $Cu(NH_3)_X^{2+}$). Accordingly,

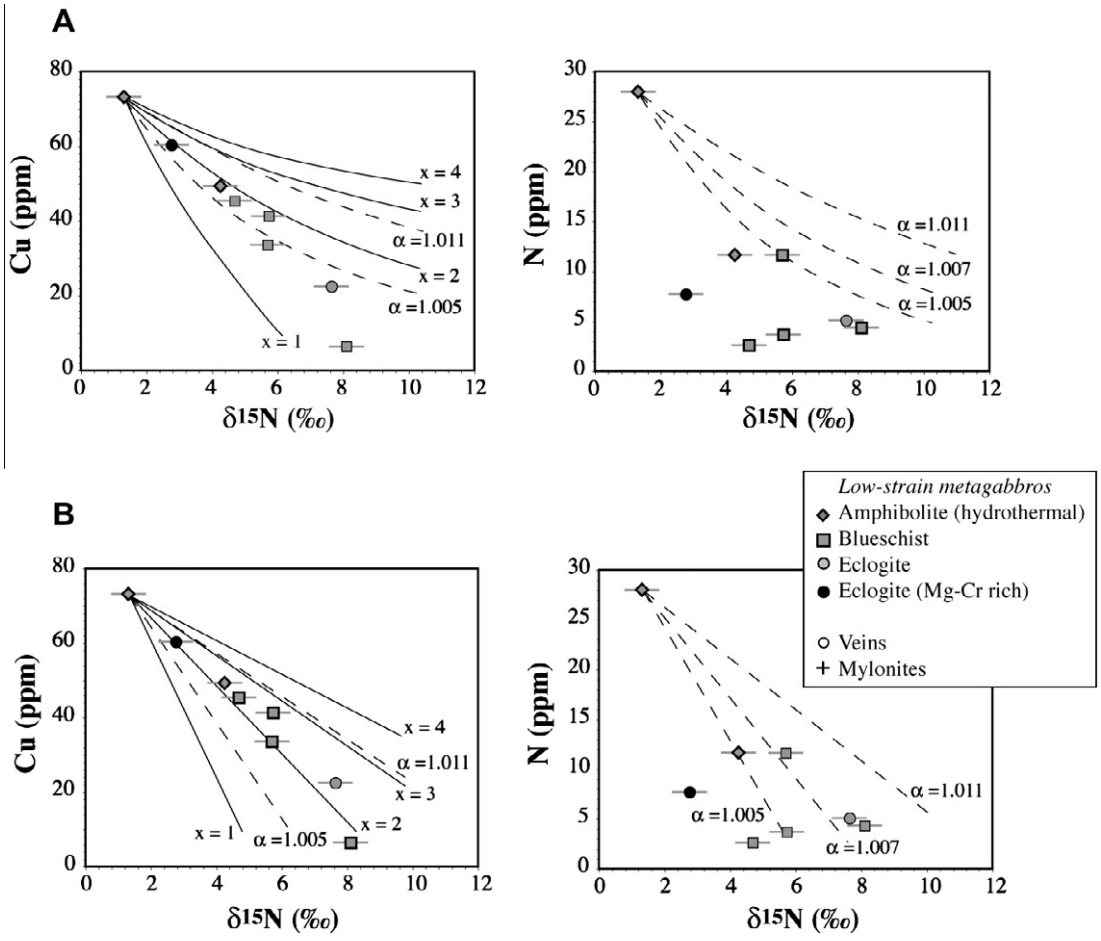

Fig. 7. Modeling of Cu and N release from the rocks during oceanic hydrothermalism. Cu and N should form a complex $Cu(NH_3)_X^{2+}$, where x is 1, 2, 3 or 4. Two models are considered: (A) Rayleigh distillation and (B) Batch equilibrium model (see main text for details of each model). Calculations are made for the different values of x and $\alpha_{NH_4-NH_3}$ (the fractionation factor between NH_4 remaining in the rock and NH_3 released in the fluid). Solid lines represent variable x values for a fixed $\alpha_{NH_4-NH_3}$ of 1.007. Dashed lines correspond to $\alpha_{NH_4-NH_3}$ of 1.005, 1.007 and 1.011 reflecting temperature of ~750, ~500, ~300 °C (Scalan, 1957; Hanschmann, 1981). In diagrams N vs $\delta^{15}N$, lines are reported only for variable $\alpha_{NH_4-NH_3}$ values because the calculated trends are not dependent on the x value (which contrasts with Cu vs $\delta^{15}N$ diagrams).

the loss of Cu and N from rock to fluid unlikely results from a Rayleigh distillation process.

In a second model, we considered that the rock and hydrothermal fluid interacted and evolved in isotope equilibrium before the fluid was expelled out of the system. Such a chemical exchange implies that the rock interacted with a same fluid phase during each step. This contrasts with the Rayleigh distillation model where the rock composition progressively evolves while interacting with different fluid aliquots that equilibrate as the reaction proceeds. The equation describing this batch equilibrium process derives from a simple isotope mass balance where the initial N present in the rock is equal to the sum of the N remaining in the rock and in the fluid phase at the end of the reaction. The equation for batch equilibrium model can be written:

$$\delta^{15}N_{NH_4} = \delta^{15}N^{0}_{NH_4} + 1000 \times F \times (\alpha - 1)$$

The results of the model are shown in Fig. 7b. The best fit of the data is obtained for $\alpha_{NH_4\text{–}NH_3} \sim 1.007$ and $x \sim 2$ giving the Cu(II) complex $Cu(NH_3)_2^{2+}$. The isotope fractionation factor $\alpha_{NH_4\text{–}NH_3}$ of ~1.007 corresponds to a temperature of ~500 °C (Scalan, 1957; Hanschmann, 1981), in good agreement with amphibolite facies conditions. Although the batch model gives a good fit on the Cu–δ^{15}N diagram, the fit is not as good on the N–δ^{15}N diagram (Fig. 7b). While initial Cu contents of the "fresh" gabbros were likely homogeneous, initial N contents may have been slightly variable (but with homogeneous δ^{15}N), for instance if the abundances of Ca–Na minerals were variable. The variability in N contents of Alpine metagabbros (Fig. 7b) would thus reflect concentration variation of the protoliths (i.e. unaltered gabbros), then modified by hydrothermal loss. In contrast, Cu contents would mostly record the hydrothermal leaching step.

We conclude that our batch equilibrium model is compatible with the present data. We note that oceanic hydrothermalism is usually considered to occur in open system (i.e. at each step, a new fluid is equilibrated with progressively evolved rock), a Rayleigh distillation would thus appear more realistic than batch equilibrium. However, Rayleigh modeling is not able to reproduce the trend observed in Cu–δ^{15}N diagram. Alpine metagabbros represent deep hydrothermalism, i.e. in the lower part of the oceanic crust, and thus likely experienced limited metamorphism with low water/rock ratio, contrasting with the upper section of the crust which may involve larger amount of fluids in open system. In order to determine if altered basalts from upper oceanic crust show the same kind of trends between Cu and δ^{15}N, we have examined data from Sites 1256 (Busigny et al., 2005a,b) and 801C (Li et al., 2007). No correlation was found for these rocks, suggesting that Cu and N geochemical relations are limited to lower crustal rocks (i.e. gabbros). The lack of correlation between Cu and δ^{15}N in altered basalts may reflect that Cu was not mobilized at low-T, contrasting with high-T process (e.g. Seewald and Seyfried, 1990).

5.3. Nitrogen and copper behavior in subducted metagabbros

Assuming that metagabbros from Chenaillet are representative analogs of the eclogitic metagabbros from Monviso, Nadeau et al. (1993) estimated the amount of water lost during eclogitization to be about 90%, which is in good agreement with results obtained from experimental data (Schmidt and Poli, 1998) and geochemical modeling (Dixon et al., 2002). The discussion presented above shows that the Cu–δ^{15}N linear correlation observed in low-strain metagabbros was inherited from a pre-subduction process, likely during oceanic hydrothermal alteration (see Section 5.2). If N would have been lost from the rocks during subduction metamorphism, isotope fractionation would have modified the rocks N isotope signature and shift them out of the initial linear correlation. Yet the preservation of the Cu–δ^{15}N correlation during subduction implies that N and Cu remained stored in low-strain metagabbros during metamorphism although eclogitization was accompanied by ~90% fluid loss. This observation is unexpected since N and Cu are usually considered as fluid-mobile elements (e.g. Seewald and Seyfried, 1990; Bebout, 1995; Heft et al., 2008). The recognition that all mylonites and veins analyzed here are located below the Cu–δ^{15}N correlation defined by low-strain metagabbros (Fig. 5d) suggests that deformation had an impact on the Cu and N geochemical behavior. This implies either that mylonites and veins have lost part of the original N and/or Cu present in low-strain rocks, or that their δ^{15}N was modified during subduction-zone metamorphism. Nitrogen loss during mylonitization or veining is unlikely because N concentrations of mylonites and veins are either similar or higher than low-strain rocks (Fig. 5a). In addition, a release of N to metamorphic fluids would produce an increase in δ^{15}N of the residual rock due to preferential partitioning of light N isotopes to the fluid phase (e.g. Haendel et al., 1986; Bebout and Fogel, 1992; Mingram and Bräuer, 2001), which is opposite to our results (Fig. 5d). On the contrary, the low Cu contents of both the veins and mylonites (<11 ppm except one at 27 ppm) compared to low-strain rocks (from 6.4 to 73.2 ppm Cu, average = 41 ± 21 ppm 2σ) indicates that part of the original Cu present in low-strain rocks was lost during mylonitization and veining. The third and last hypothesis to be considered is a modification of δ^{15}N values due to an external source. If the Cu concentrations of veins and mylonites are considered similar to the original low-strain rocks, then an interaction with a N-bearing fluid depleted in heavy isotope is required. N_2- or NH_3-bearing fluids released from dehydration of crustal rocks are systematically depleted in heavy isotope relative to their host rock, being sedimentary, mafic (gabbros, basalts) or ultramafic (serpentine) in origin (e.g. Haendel et al., 1986; Bebout and Fogel, 1992; Mingram and Bräuer, 2001). The high N content of vein VS–14V (55 ppm) compared to other eclogite facies samples (<28 ppm N) strongly suggests that a fraction of the N carried in the veins may have been brought to the rock by external fluids. The presence of K in two of the veins investigated further supports that an externally-derived fluid phase carrying K and N infiltrated Monviso eclogite facies rocks at some stage of their HP metamorphic history. The slight K- and N- enrichment may point towards a sedimentary source rather than a mafic or ultramafic origin. Considering that the veins and mylonites were affected by an external N-bearing fluid, it is interesting to note that their δ^{15}N values show a large range of variation (from 0.8‰

to 5.9‰). This implies that either (1) several fluids with various $\delta^{15}N$ values infiltrated the metagabbros and imprinted their geochemical signatures, or more likely that (2) N in mylonites and veins represent a mixing between N initially present in the rocks before subduction (with variable $\delta^{15}N$) and N derived from external fluids (with homogeneous and light $\delta^{15}N$).

To summarize, mylonites and veins have experienced either some loss of Cu and/or metasomatism by external fluids bearing ^{15}N-depleted nitrogen. The present data suggest that, during eclogitization, N and Cu were affected by dynamic deformation of the rocks while static recrystallization favored their preservation into mineral structures.

5.4. Implication for nitrogen recycling from Earth surface to the deep mantle

The present work is the first to provide N content and isotope data on a suite of metagabbros. These rocks are broadly representative of the oceanic crust formed at ridge axes in modern divergent margins, hydrothermally-altered by seawater-derived fluids and subducted in a cold slab environment typical of present day settings (Peacock, 1996). However, it must be noted that the western Alps Jurassic ophiolites are usually regarded as being more "Atlantic-type" crustal sections in which rocks such as gabbros and even serpentinites are present near the top of the ophiolitic section and likely more vulnerable to seawater–rock interactions (e.g. Lagabrielle and Cannat, 1990). The "Pacific-type" oceanic crust thought to be subducting into most of Earth's modern subduction zones in contrast shows the preservation of the pillow basalt section, at the top of the crust, and the gabbroic section may experience degrees of seafloor alteration smaller than those experienced in the "Atlantic-type" settings. Thus, western Alps metagabbros may have experienced greater water–rock interaction, and thus greater loss of N during high temperature hydrothermalism, than typical lower crust buried in modern subduction zones. This question is difficult to solve since the gabbroic section of the Pacific oceanic crust is still poorly known. Only recently the first sequence of an intact oceanic crust has been drilled from the lava, through the sheeted dike complex, down to the gabbros (Wilson et al., 2006), but its N content and isotope composition has not been analyzed yet. In the following discussion, we will assume that Alpine metagabbros are representative of lower crustal gabbros buried into modern subduction zones and we will use the present data to estimate average N concentrations and isotope composition of subducting metagabbros. A previous study of the Monviso metagabbros estimated that low-strain rocks and mylonites represent ~98% of the subducting metagabbros, while only 2% of the metagabbros correspond to veins (Philippot and van Roermund, 1992). Because veins are negligible in proportion (2%), and their N concentrations are strongly variable, we have estimated average N content and isotope composition based on low-strain rocks and mylonites only, that is 10.6 ± 5.1 ppm and $+1.8 \pm 0.8$‰ (1σ, $n = 11$), respectively.

The fluxes of N input in subduction zones by the various components of the oceanic crust are listed in Table 5. The flux of N carried by serpentinized peridotites is so far neglected because the mass flux of subducted serpentinites is presently underconstrained (see Philippot et al., 2007). Metagabbros are a major component of the subducted oceanic crust, with a flux of $\sim 4 \times 10^{16}$ g/yr (Peacock, 1990), twice that of basaltic crust. Considering the mean N content of mylonites and low-strain metagabbros calculated in this study, the flux of N subducted by metagabbros is estimated at 4.2 (± 2.0) $\times 10^{11}$ g/yr. We acknowledge that this estimate is based on a limited amount of data and that further study might lead to slightly different budget but first-order conclusions can be drawn. This value is half

Table 5
Nitrogen fluxes exchanged between internal and external reservoirs of the Earth.

	Total flux (g/yr)	[N] (ppm)	1σ	N flux (g/yr)	$\delta^{15}N$ (‰)	1σ
Input fluxes						
Sediments	1.8×10^{15}[a]	424	±33	7.6×10^{11}	+4.1[f]	±1.6
Upper crust (basalts)	2.0×10^{16}[b]	6.5	±2.6	1.3×10^{11}	+4.7	±2.4
Lower crust (gabbros)	4.0×10^{16}[b]	5.9	±3.0	4.2×10^{11}	+1.8	±0.8
Total input flux				13.2×10^{11}	+3.4	±1.4
Output fluxes						
Mid-ocean ridges	–	–	–	0.7×10^{11}[c]	−5.0	±2.0
Intraplate volcanism	–	–	–	5.7×10^{7}[d]	–	–
Arc volcanism	–	–	–	2.8×10^{11}[e]	–	–
Back-arc basins	–	–	–	7.8×10^{9}[d]	–	–
Total output flux				3.6×10^{11}		

For input fluxes, we provide total mass flux, average N concentration, flux of N subducted and average $\delta^{15}N$ for each component of the subducting oceanic crust.

[a] Plank and Langmuir (1998).

[b] Peacock (1990).

[c] Estimated from N/He/Ar, C/N, mantle C-fluxes and C/Nb systematics after Cartigny et al. (2008) and data from Marty (1995), Javoy and Pineau (1991), Saal et al. (2002).

[d] Sano et al. (2001).

[e] Hilton et al. (2002).

[f] Estimate from a personal compilation (see Chapter II in Busigny, 2004).

the sedimentary N flux input in subduction zones estimated for comparable geotherms (7.6×10^{11} g/yr; Busigny et al., 2003a), showing that gabbros represent a significant source of N recycling to the mantle. The contribution of the basaltic portion to the deeply subducted lithosphere can be estimated from data on basaltic eclogites. Eclogites from Raspas Complex (Ecuador), with elevated $\delta^{18}O$ (Halama et al., 2011), and from Lago di Cignana (Italy), with relic pillow structure (van der Klauw et al., 1997; Reinecke, 1998), are identified as metabasalts. These eclogites have a relatively restricted range of N content and $\delta^{15}N$, with an average of 6.5 ± 2.6 ppm and $+4.7 \pm 2.4‰$, respectively (1σ, $n = 19$, excepting one sample with particularly high N content; Halama et al., 2010). Considering the mass flux of the upper basaltic crust buried in subduction zones is $\sim 2 \times 10^{16}$ g/yr, the flux of N carried by the upper oceanic crust is about $1.3 (\pm 0.5) \times 10^{11}$ g/yr.

Fluxes input to subduction zones are compared to the fluxes of N output from the mantle by mid-ocean ridges, intraplate volcanism, arc volcanism and back-arc basins in Table 5 (see Section 1 for a detailed description of the fluxes). The total flux of N input in subduction zones (13.2×10^{11} g/yr) is almost five times higher than the flux of N output from arc volcanism (2.8×10^{11} g/yr; Hilton et al., 2002). Thus, about 80% of the N input is transferred to the mantle and not recycled to the surface (Table 5). This result is in good agreement with recent findings that N is massively cycled to the deep mantle in subduction zone environment (Busigny et al., 2003a,2005a,b; Sadofsky and Bebout, 2003; Li and Bebout, 2005; Li et al., 2007; Halama et al., 2010; Mitchell et al., 2010) and contrasts with early conclusions from the study of Central America subduction zones, in which a biased subduction budget was considered (Fischer et al., 2002; for a complete subduction budget see Li and Bebout, 2005; Li et al., 2007). A more recent study of volcanic gases in the Central America recognized the contribution of altered oceanic crust and proposed that N output flux from the arc may represent only 42% of the total input flux (Elkins et al., 2006). Accordingly, all detailed and recent studies confirm that a large portion of the N input in subduction zones is transferred to the deep mantle. When compared to the total flux of N output from the mantle, including mid-ocean ridges, arc volcanism, back-arc basins and intraplate volcanism (3.6×10^{11} g/yr), the total flux of N input in subduction zone is still significantly higher (more than three times higher). This implies that N contained in Earth surface reservoirs (mainly atmosphere but also hydrosphere, biosphere and crust) is progressively transferred and sequestered into the mantle, with a net flux of N input at $\sim 9.6 \times 10^{11}$ g/yr. Assuming a constant flux through time, the total amount of N present in the atmosphere (3.98×10^{21} g) could be sequestered in ~4.15 Ga. This net flux of N input to the mantle is thus insufficient to change significantly the amount of atmospheric N over a period shorter than 500 Ma.

Our flux estimates can also be used to constrain the past N distribution between atmosphere and mantle reservoirs. In particular, we can test the proposal of a recent study by Goldblatt et al. (2009), suggesting that (i) early Earth atmosphere contained twice as much N as today and (ii) during the first 2 Ga of the Earth history, half of this initial atmospheric N has been sequestered into the silicate Earth by way of subduction. This model was proposed to solve the so-called "faint young sun paradox", i.e. the paradox of a non-permanent glaciated early Earth despite a poorly energetic young sun. A major uncertainty in this model is that early subduction fluxes are largely unknown. Goldblatt et al. (2009) considered that the tectonic cycling was much more active, with a higher input flux than in modern subduction zones. However, they neglected that: (i) the flux of N output from volcanism was likely higher than the modern one (due to more active tectonics), (ii) the geothermal gradient in subduction zones was higher in the past than today and thus, a large amount of volatiles was likely released and not recycled to the deep mantle (i.e. low input flux; Bebout et al., 1999; Busigny et al., 2003a), and (iii) typical Archean marine sediments (i.e. Banded Iron Formations) contain a very small amount of N (few ppm; e.g. Beaumont and Robert, 1999; Pinti et al., 2001) relative to modern marine sediments buried in subduction zones (few hundreds of ppm). Although Archean shales contain similar N concentrations than modern sediments (e.g. Jia and Kerrich, 2004b; Garvin et al., 2009), they were likely deposited in "coastal settings" and it is unclear whether these were recycled into subduction zones. Overall, we can reasonably consider that the ancient flux of subducted N was similar to or smaller than the modern one. Assuming that early Earth atmosphere contained twice as much N as today (i.e. $\sim 8 \times 10^{21}$ g; Goldblatt et al., 2009), a constant flux of subducted N over the Earth's history ($\sim 9.6 \times 10^{11}$ g/yr) implies that only 1/4 of the early atmospheric N amount would have been sequestered into the silicate Earth over a period of 2 Ga. Accordingly, 50% of an early N_2-rich atmosphere cannot have been sequestered in the first 2 Ga of Earth's history as suggested by Goldblatt et al. (2009), since it requires at least 4 Ga of subduction entrapment, even with the highest recycling fluxes considered above.

6. CONCLUSIONS

In the present work, we have examined typical oceanic gabbros, hydrothermalized by seawater-derived fluids, and then subducted along a low geothermal gradient (~8 °C/km). We find an inverse linear correlation between Cu and $\delta^{15}N$ for low-strain metagabbros, which indicates, together with major and trace element data, that Cu and N geochemistry have been coupled during the formation and/or evolution of these gabbros. This correlation is incompatible with either a syn-subduction process or magmatic differentiation but rather derives from oceanic hydrothermal alteration. We predict that other altered gabbros would display such Cu–$\delta^{15}N$ relationship, while unaltered equivalents would not.

The preservation of Cu–$\delta^{15}N$ linear correlation for low-strain metagabbros implies that static metamorphism associated to subduction did not affect significantly nitrogen and copper. Nitrogen and copper of subducting metagabbros can thus be preserved to P–T conditions of 2.5 GPa and 500 °C. However, the study of mylonites and veins indicates that pervasive ductile deformation and veining affected the

primary signal, which was associated with a release of Cu in fluids and/or a metasomatic addition of N by external fluids.

Considerations about global N budget confirm a large recycling to the deep mantle in subduction zones. Massive recycling may have imparted significant modifications of the N content and isotope composition in the Earth mantle and possibly atmosphere over geological time.

ACKNOWLEDGMENTS

Colleagues from the Isotope Geochemistry Laboratories in IPGP are thanked for fruitful discussions, particularly Jabrane Labidi, Jean-Louis Birck and Marc Javoy. Michel Girard, Jean-Jacques Bourrand and Guillaume Landais are acknowledged for their technical assistance. Marc Quintin is thanked for making thin sections of all samples. Philippe Agard is thanked for discussions and providing a map from the Western Alps. Gray Bebout, Ralf Halama and Long Li are thanked for their careful and detailed reviews. Jeff Alt is greatly acknowledged for handling and reviewing the manuscript.

REFERENCES

Ader M., Cartigny P., Boudou J.-P., Oh J.-H., Petit E. and Javoy M. (2006) Nitrogen isotopic evolution of carbonaceous matter during metamorphism: methodology and preliminary results. *Chem. Geol.* **232**, 152–169.

Agard P., Jolivet L. and Goffé B. (2001) Tectonometamorphic evolution of the Schistes Lustrés complex: implications for the exhumation of HP and UHP rocks in the western Alps. *Bull. Soc. Géol. Fr.* **5**, 617–636.

Alirezaei S. and Cameron E. M. (2002) Mass balance during gabbro-amphibolite transition, Bamble Sector, Norway: implications for petrogenesis and tectonic setting of the gabbros. *Lithos* **60**, 21–45.

Alt J. C. (1995) Subseafloor processes in mid-ocean ridge hydrothermal systems. In *Seafloor Hydrothermal Systems: Physical, Chemical, and Biological Interactions* (eds. S. Humphris, J. Lupton, L. Mullineaux and R. Zierenberg). Geophysical Monograph 91, AGU, Washington DC, pp. 85–114.

Alt J. C. and Anderson T. F. (1991) The mineralogy and isotopic composition of sulfur in Layer 3 gabbros from the Indian Ocean, ODP Hole 735B. *Proc. ODP, Scientific Results* **118**, 113–125.

Alt J. C. and Teagle D. A. H. (2003) Hydrothermal alteration of upper oceanic crust formed at fast-spreading ridge: mineral, chemical, and isotopic evidence from ODP Site 801. *Chem. Geol.* **201**, 191–211.

Beaumont V. and Robert F. (1999) Nitrogen isotope ratios of kerogens in Precambrian cherts: a record of the evolution of atmosphere chemistry. *Precambrian Res.* **96**, 63–82.

Bebout G. E. (1995) The impact of subduction-zone metamorphism on mantle-ocean chemical cycling. *Chem. Geol.* **126**, 191–218.

Bebout G. E. and Fogel M. L. (1992) Nitrogen-isotope compositions of metasedimentary rocks in the Catalina Schist, California: implications for metamorphic devolatilization history. *Geochim. Cosmochim. Acta* **56**, 2839–2849.

Bebout G. E., Ryan J. G., Leeman W. P. and Bebout A. E. (1999) Fractionation of trace elements by subduction-zone metamorphism – effect of convergent-margin thermal evolution. *Earth Planet. Sci. Lett.* **171**, 63–81.

Beran A., Armstrong J. and Rossman G. R. (1992) Infrared and electron microprobe analysis of ammonium ions in hyalophane feldspar. *Eur. J. Mineral.* **4**, 847–850.

Bjerrum J. (1941) *Metal ammine formation in aqueous solutions*. P. Haase and Son, Copenhagen, Denmark, 296pp..

Bottrell S. H., Carr L. P. and Dubessy J. (1988) A nitrogen-rich metamorphic fluid and coexisting minerals in slates from North Wales. *Mineral. Mag.* **52**, 451–457.

Boyd S. R. and Pillinger C. T. (1994) A preliminary study 15N/14N in octahedral growth form diamonds. *Chem. Geol.* **116**, 43–59.

Boyd S. R. and Philippot P. (1998) Precambrian ammonium biogeochemistry: a study of the Moine metasediments, Scotland. *Chem. Geol.* **144**, 257–268.

Brügmann G. E., Naldrett A. J., Asif M., Lightfoot P. C., Gorbatchev N. S. and Fedorenko V. A. (1993) Siderophile and chalcophile metals as traces of the evolution of the Siberian Trap in the Noril'sk region, Russia. *Geochim. Cosmochim. Acta* **57**, 2001–2018.

Busigny V. (2004) Comportement geochimique de l'azote dans les zones de subduction. Ph. D. dissertation, University Paris Diderot, Paris, France.

Busigny V., Cartigny P., Philippot P., Ader M. and Javoy M. (2003a) Massive recycling of nitrogen and other fluid-mobile elements (K, Rb, Cs, H) in a cold slab environment: evidences from HP to UHP oceanic metasediments of the Schistes Lustrés nappe (Western Alps, Europe). *Earth Planet. Sci. Lett.* **215**, 27–42.

Busigny V., Cartigny P., Philippot P. and Javoy M. (2003b) Ammonium quantification in muscovite by infrared spectroscopy. *Chem. Geol.* **198**, 21–31.

Busigny V., Cartigny P., Philippot P. and Javoy M. (2004) Quantitative analysis of ammonium in biotite using infrared spectroscopy. *Am. Mineral.* **89**, 1625–1630.

Busigny V., Laverne C. and Bonifacie M. (2005a) Nitrogen content and isotopic composition of oceanic crust at a superfast spreading ridge: a profile in altered basalts from ODP Site 1256, Leg 206. *Geochem. Geophys. Geosyst.* **6**, Q12O01. doi:10.1029/2005GC001020.

Busigny V., Ader M. and Cartigny P. (2005b) Quantification and isotopic analysis of nitrogen in rocks at the ppm level using sealed-tube combustion technique: a prelude to the study of altered oceanic crust. *Chem. Geol.* **223**, 249–258.

Cartigny P., Boyd S. R., Harris J. W. and Javoy M. (1997) Nitrogen isotopes in peridotitic diamonds from Fuxian, China: The mantle signature. *Terra Nova* **9**, 175–179.

Cartigny P., De Corte K., Shatsky V. S., Ader M., De Paepe P., Sobolev N. V. and Javoy M. (2001a) The origin and formation of metamorphic microdiamonds from the Kokchetav massif, Kazakhstan: a nitrogen and carbon isotopic study. *Chem. Geol.* **176**, 265–281.

Cartigny P., Jendrzejewski N., Pineau F., Petit E. and Javoy M. (2001b) Volatile (C, N, Ar) variability in MORB and the respective role of mantle source heterogeneity and degassing: the case of the Southwest Indian Ridge. *Earth Planet. Sci. Lett.* **194**, 241–257.

Cartigny P., Pineau F., Aubaud C. and Javoy M. (2008) Towards a consistent mantle carbon flux estimate: Insights from volatile systematics (H_2O/Ce, dD, CO_2/Nb) in the North Atlantic mantle (14°N and 34°N). *Earth Planet. Sci. Lett.* **265**, 672–685.

Dixon J. E., Leist L., Langmuir C. and Schilling J.-G. (2002) Recycled dehydrated lithosphere observed in plume-influenced mid-ocean-ridge basalt. *Nature* **420**, 385–389.

Elkins L. J., Fischer T. P., Hilton D. R., Sharp Z. D., McKnight S. and Walker J. (2006) Tracing nitrogen in volcanic and geothermal volatiles from the Nicaraguan volcanic front. *Geochim. Cosmochim. Acta* **70**, 5215–5235.

Fischer T. P., Hilton D. R., Zimmer M. M., Shaw A. M., Sharp Z. D. and Walker J. A. (2002) Subduction and recycling of nitrogen along the Central American margin. *Science* **297**, 1154–1157.

Gallien J.-P., Orberger B., Daudin L., Pinti D. L. and Pasava J. (2004) Nitrogen in biogenic and abiogenic minerals from Paleozoic black shales: an NRA study. *Nucl. Instrum. Methods Phys. Res., Sect. B* **217**, 113–122.

Garvin J., Buick R., Anbar A., Arnold G. L. and Kaufman A. J. (2009) Isotopic evidence for an aerobic nitrogen cycle in the latest Archean. *Science* **323**, 1045–1048.

Goldblatt C., Claire M. W., Lenton T. M., Matthews A. J., Watson A. J. and Zahnle K. (2009) Nitrogen-enhanced greenhouse warming on early Earth. *Nat. Geosci.* **2**, 891–896.

Haendel D., Mühle K., Nitzsche H., Stiehl G. and Wand U. (1986) Isotopic variations of the fixed nitrogen in metamorphic rocks. *Geochim. Cosmochim. Acta* **50**, 749–758.

Halama R., Bebout G. E., John T. and Schenk V. (2010) Nitrogen recycling in subducted oceanic lithosphere: the record in high- and ultrahigh-pressure metabasaltic rocks. *Geochim. Cosmochim. Acta* **74**, 1636–1652.

Halama R., John T., Herms P., Hauff F. and Schenk V. (2011) A stable (Li, O) and radiogenic (Sr, Nd) isotope perspective on metasomatic processes in a subducting slab. *Chem. Geol.* **281**, 151–166.

Hamlyn P. R., Keays R. R., Cameron W. E., Crawford A. J. and Waldron H. M. (1985) Precious metals in magnesian low-Ti lavas: implications for metallogenesis and sulfur saturation in primary magmas. *Geochim. Cosmochim. Acta* **49**, 1797–1811.

Hanschmann G. (1981) Berechnung von isotopieeffekten auf quantenchmischer grundlage am beispiel stickstoff fhaltiger moleküle. *Zfl.-Mitt.* **41**, 19–39.

Hashizume K., Chaussidon M., Marty B. and Robert F. (2000) Solar wind record on the Moon: deciphering presolar from planetary nitrogen. *Science* **290**, 1142–1145.

Heft K. L., Gillis K. M., Pollock M. A., Karson J. A. and Klein E. M. (2008) Role of upwelling hydrothermal fluids in the development of alteration patterns at fast spreading ridges: evidence from the sheeted dike complex at Pito Deep. *Geochem. Geophys. Geosyst.* **9**, Q05O07. doi:10.1029/2007GC001926.

Hilton D. R., Fischer T. P. and Marty B. (2002) Noble gases and volatile recycling at subduction zones. In *Noble Gases in Geochemistry and Cosmochemistry* (eds. D. Porcelli, C. J. Ballentine and R. Wieler). Rev. Mineral. Geochem 47, Washington DC, pp. 319–370.

Honma H. and Itihara Y. (1981) Distribution of ammonium in minerals of metamorphic and granitic rocks. *Geochim. Cosmochim. Acta* **45**, 983–988.

Javoy M. (1998) The birth of the Earth's atmosphere: the behaviour and fate of its major elements. *Chem. Geol.* **147**, 11–25.

Javoy M. and Pineau F. (1991) The volatiles record of a "popping" rock from the Mid-Atlantic ridge at 14°N: chemical and isotopic composition of gas trapped in the vesicules. *Earth Planet. Sci. Lett.* **107**, 598–611.

Javoy M., Pineau F. and Demaiffe D. (1984) Nitrogen and carbon isotopic composition in the diamonds of Mbuji Mayi (Zaïre). *Earth Planet. Sci. Lett.* **68**, 399–412.

Jia Y. and Kerrich R. (2004a) A reinterpretation of the crustal N-isotope record: evidence for a 15N-enriched Archean atmosphere? *Terra Nova* **16**, 102–108.

Jia Y. and Kerrich R. (2004b) Nitrogen 15-enriched Precambrian kerogen and hydrothermal systems. *Geochem. Geophys. Geosyst.* **5**, Q07005. doi:10.1029/2004GC000716.

Kendall C. and Grim E. (1990) Combustion tube method for measurement of nitrogen isotope ratios using calcium oxide for total removal of carbon dioxide and water. *Anal. Chem.* **62**, 525–529.

Lagabrielle Y. and Cannat M. (1990) Alpine Jurassic ophiolites resemble the modern central Atlantic basement. *Geology* **18**, 319–322.

Libourel G., Marty B. and Humbert F. (2003) Nitrogen solubility in basaltic melt. Part I. Effect of oxygen fugacity. *Geochim. Cosmochim. Acta* **67**, 4123–4135.

Li L. and Bebout G. E. (2005) Carbon and nitrogen geochemistry of sediments in the Central American convergent margin: insights regarding subduction input fluxes, diagenesis, and paleoproductivity. *J. Geophys. Res.* **110**, B11202. doi:10.1029/2004JB003276.

Li L., Bebout G. E. and Idleman B. D. (2007) Nitrogen concentration and $d^{15}N$ of altered oceanic crust obtained on ODP Legs 129 and 185: insights into alteration-related nitrogen enrichment and the nitrogen subduction budget. *Geochim. Cosmochim. Acta* **71**, 2344–2360.

Le Pichon X., Bergerat F. and Roulet M. J. (1988) Plate kinematics and tectonics leading to the Alpine belt formation: a new analysis. *Geol. Soc. Am.* **218**, 111–131.

Lombardo B., Nervo R., Compagnoni R., Messiga B., Kienast J. R., Mével C., Fiora L., Piccardo G. B. and Lanza R. (1978) Osservazioni preliminari sulle ofioliti metamorphiche del Monviso (Alpi Occidentali). *Rendiconti della Soc. Ital. Mineral. Petrol.* **34**, 253–305.

Manatschal G., Sauter D., Karpoff A. M., Masini E., Mohn G. and Lagabrielle Y. (2011) The Chenaillet ophiolite in the French/Italian Alps: an ancient analogue for oceanic core complex? *Lithos* **124**, 169–184.

Mével C., Caby R. and Kienast J.-R. (1978) Amphibolite facies conditions in the oceanic crust: example of amphibolized flaser-gabbro and amphibolites from the Chenaillet ophiolite massif (Hautes Alpes, France). *Earth Planet. Sci. Lett.* **39**, 98–108.

Marty B. (1995) Nitrogen content of the mantle inferred from N_2–Ar correlation in oceanic basalts. *Nature* **377**, 326–329.

Marty B. and Dauphas N. (2003) The nitrogen record of crust–mantle interaction and mantle convection from Archean to Present. *Earth Planet. Sci. Lett.* **206**, 397–410.

Marty B. and Humbert F. (1997) Nitrogen and argon isotopes in oceanic basalts. *Earth Planet. Sci. Lett.* **152**, 101–112.

Marty B. and Zimmermann L. (1999) Volatiles (He, C, N, Ar) in mid-ocean ridge basalts: assesment of shallow-level fractionation and characterization of source composition. *Geochim. Cosmochim. Acta* **63**, 3619–3633.

Messiga B., Kienast J. R., Rebay G., Piccardi P. and Tribuzio R. (1999) Cr-rich magnesiochloritoid eclogites from the Monviso ophiolites (Western Alps, Italy). *J. Metamophic Geol.* **17**, 287–299.

Mingram B. and Bräuer K. (2001) Ammonium concentration and nitrogen isotope composition in metasedimentary rocks from different tectonometamorphic units of the European Variscan Belt. *Geochim. Cosmochim. Acta* **65**, 273–287.

Mitchell E. C., Fischer T. P., Hilton D. R., Hauri E. H. and Shaw A. M., et al. (2010) Nitrogen sources and recyling at subduction zones: Insights from the Izu-Bonin-Mariana arc. *Geochem. Geophys. Geosys.* **11**, Q02X11. doi:10.1029/2009GC002783.

Monié P. and Philippot P. (1989) Mise en évidence de l'âge éocène moyen du métamorphisme de haute-pression dans la nappe éclogitique du Monviso (Alpes Occidentales) par la méthode ^{39}Ar–^{40}Ar. *C. R. Acad. Sci.* **309**, 245–251.

Mysen B. and Fogel M. (2010) Nitrogen and hydrogen isotope compositions and solubility in silicate melts in equilibrium with reduced (N+H)-bearing fluids at high pressure and temperature: effects of melt structure. *Am. Mineral.* **95**, 987–999.

Mysen B., Yamashita S. and Chertkova N. (2008) Solubility and solution mechanisms of NOH volatiles in silicate melts at high pressure and temperature – amine groups and hydrogen fugacity. *Am. Mineral.* **93**, 1760–1770.

Nadeau S., Philippot P. and Pineau F. (1993) Fluid inclusion and mineral isotopic compositions (H–C–O) in eclogitic rocks as tracers of local fluid migration during high-pressure metamorphism. *Earth Planet. Sci. Lett.* **114**, 431–448.

Olofsson G. (1975) Thermodynamic quantities for the dissociation of the ammonium ion and for the ionization of aqueous ammonia over a wide temperature range. *J. Chem. Thermodyn.* **7**, 507–514.

Orberger B., Gallien J.-P., Pinti D. L., Fialin M., Daudin L., Gröcke D. R. and Pasava J. (2005) Nitrogen and carbon partitioning in diagenetic and hydrothermal minerals from Paleozoic black shales (Selwyn Basin, Yukon Territories, Canada). *Chem. Geol.* **218**, 249–264.

Palya A. P., Buick I. S. and Bebout G. E. (2011) Storage and mobility of nitrogen in the continental crust: Evidence from partially meted metasedimentary rocks, Mt. Stafford, Australia. *Chem. Geol.* **281**, 211–226.

Peacock S. M. (1990) Fluid processes in subduction zones. *Science* **248**, 329–336.

Peacock S. M. (1996) Thermal and petrologic structure of subduction zones. In *Subduction: Top to Bottom* (eds. G. E. Bebout, D. W. Scholl, S. H. Kirby and J. P. Platt). Geophysical Monograph 96, AGU, Washington DC, pp. 119–133.

Pinti D. L., Hashizume K. and Matshuda J. (2001) Nitrogen and argon signatures in 3.8 to 2.8 Ga metasediments: clues on the chemical state of the Archean ocean and the deep biosphere. *Geochim. Cosmochim. Acta* **65**, 2301–2315.

Philippot P. (1987) "Crack seal" vein geometry in eclogitic rocks. *Geodin. Acta* **1**, 171–181.

Philippot P. (1993) Fluid–melt–rock interaction in mafic eclogites and coesite-bearing metasediments: constraints on volatile recycling during subduction. *Chem. Geol.* **108**, 93–112.

Philippot P. and Kienast J. R. (1989) Chemical-microstructural changes in eclogite-facies shear zones (Monviso, Western Alps, north Italy) as indicators of strain history and the mechanism and scale of mass transfer. *Lithos* **23**, 179–200.

Philippot P. and Selverstone J. (1991) Trace-element-rich brines in eclogitic veins: implications for fluid composition and transport during subduction. *Contrib. Mineral. Petrol.* **106**, 417–430.

Philippot P. and van Roermund H. L. M. (1992) Deformation processes in eclogitic rocks: evidence for the rheological delamination of the oceanic crust in deeper level of subduction zones. *J. Struct. Geol.* **14**, 1059–1077.

Philippot P., Agrinier P. and Scambelluri M. (1998) Chlorine cycling during subduction of altered oceanic crust. *Earth Planet. Sci. Lett.* **161**, 33–44.

Philippot P., Busigny V., Scambelluri M. and Cartigny P. (2007) Nitrogen and oxygen isotopes as tracers of fluid activities in serpentinites and metasediments during subduction. *Mineral. Petrol.* **91**, 11–24.

Pitcairn I. K., Teagle D. A. H., Kerrich R., Craw D. and Brewer T. S. (2005) The behavior of nitrogen and nitrogen isotopes during metamorphism and mineralization: evidence from the Otago and Alpine Schists, New Zealand. *Earth Planet. Sci. Lett.* **233**, 229–246.

Plank T. and Langmuir C. H. (1998) The chemical composition of subducting sediment and its consequences for the crust and mantle. *Chem. Geol.* **145**, 325–394.

Reinecke T. (1998) Prograde high- to ultrahigh-pressure metamorphism and exhumation of oceanic sediments at Lago di Cignana, Zermatt-Saas Zone, western Alps. *Lithos* **42**, 147–189.

Richet P., Bottinga Y. and Javoy M. (1977) A review of hydrogen, carbon, nitrogen, oxygen, sulphur and chlorine stable isotope fractionation among gaseous molecules. *Ann. Rev. Earth Planet.* **5**, 65–110.

Roskosz M., Mysen B. and Cody G. D. (2006) Dual speciation of nitrogen in silicate melts at high pressure and temperature: an experimental study. *Geochim. Cosmochim. Acta* **70**, 2902–2918.

Sadofsky S. J. and Bebout G. E. (2003) Record of forearc devolatilization in low-T, high-P/T metasedimentary suites: significance for models of convergent margin chemical cycling. *Geochem. Geophys. Geosyst.* **4**, 9003. doi:10.1029/2002GC000412.

Saal A. E., Hauri E. H., Langmuir C. H. and Perfit M. R. (2002) Vapour undersaturation in primitive mid-ocean-ridge basalt and the volatile content of Earth's upper mantle. *Nature* **419**, 451–455.

Sano Y. and Pillinger C. T. (1990) Nitrogen isotopes and N/Ar ratios in cherts: an attempt to measure time evolution of atmospheric $d^{15}N$ value. *Geochem. J.* **24**, 315–325.

Sano Y., Takahata N., Nishio Y., Fischer T. P. and Williams S. N. (2001) Volcanic flux of nitrogen from the Earth. *Chem. Geol.* **171**, 263–271.

Scalan R. S. (1957) The isotopic composition, concentration, and chemical state of the nitrogen in igneous rocks. Ph. D dissertation. University of Arkansas.

Schmidt M. W. and Poli S. (1998) Experimentally based water budgets for dehydrating slabs and consequences for arc magma generation. *Earth Planet. Sci. Lett.* **163**, 361–379.

Seewald J. S. and Seyfried, Jr., W. E. (1990) The effect of temperature on metal mobility in subseafloor hydrothermal systems: constraints from basalt alteration experiments. *Sci. Lett.* **101**, 388–403.

Spandler C., Hermann J., Arculus R. and Mavrogenes J. (2004) Geochemical heterogeneity and element mobility in deeply subducted oceanic crust; insight from high-pressure mafic rocks from New Caledonia. *Chem. Geol.* **206**, 21–42.

Staudigel H. (2003) Hydrothermal alteration processes. In *The Crust. Treatise on Geochemistry*, vol. 3 (eds. H. Holland and K. Turekian). Elsevier, New York, pp. 511–535.

Tolstikhin I. N. and Marty B. (1998) The evolution of terrestrial volatiles: a view from helium, neon, argon and nitrogen isotope modelling. *Chem. Geol.* **147**, 27–52.

Thomazo C., Pinti D. L., Busigny V., Ader M., Hashizume K. and Philippot P. (2009) Biological activity and the Earth's surface evolution: insights from carbon, sulfur, nitrogen and iron stable isotopes in the rock record. *C. R. Palevol.* **8**, 665–678.

Thomazo C., Ader M. and Philippot P. (2010) Extreme ^{15}N-enrichments in 2.72-Gyr-old sediments: evidence for a turning point in the nitrogen cycle. *Geobiology* **9**, 107–120.

Van der Klauw S. N. G. C., Reinecke T. and Stöckhert B. (1997) Exhumation of ultrahigh-pressure metamorphic crust fromL-ago di Cignana, Piemontese zone, western Alps: the structural record in metabasites. *Lithos* **41**, 79–102.

Vedder W. (1964) Correlations between infrared spectrum and chemical composition of mica. *Am. Mineral.* **49**, 736–768.

Vedder W. (1965) Ammonium in muscovite. *Geochim. Cosmochim. Acta* **29**, 221–228.

Watenphul A., Wunder B. and Heinrich W. (2009) High-pressure ammonium-bearing silicates: implications for nitrogen and hydrogen storage in the Earth's mantle. *Am. Mineral.* **94**, 283–292.

Watenphul A., Wunder B., Wirth R. and Heinrich W. (2010) Ammonium-bearing clinopyroxene: a potential nitrogen reservoir in the Earth's mantle. *Chem. Geol.* **270**, 240–248.

Wedepohl K. H. (1995) The composition of the continental crust. *Geochim. Cosmochim. Acta* **59**, 1217–1232.

Wilson D. S., Teagle D. A. H., Alt J. C., Banerjee N. R. and Umino S., et al. (2006) Drilling to gabbro in intact ocean crust. Drilling to gabbro in intact ocean crust. *Science* **312**, 1016–1020.

Yamamoto T. and Nakahira M. (1966) Ammonium in sericites. *Am. Mineral.* **51**, 1775–1787.

Yardley B. W. D., Banks D. A., Bottrell S. H. and Diamond L. W. (1993) Post-metamorphic gold-quartz veins from N.W. Italy: the composition and origin of the ore fluid. *Mineral. Mag.* **57**, 407–422.

Yokochi R., Marty B., Chazot G. and Burnard P. (2009) Nitrogen in peridotite xenoliths: lithophile behavior and magmatic isotope fractionation. *Cosmochim. Acta* **73**, 4843–4861.

Associate editor: Jeffrey C. Alt